Advances in Differential Equations and Control Processes 2025, 32(2), 2873.
https://doi.org/10.59400/adecp2873

Article

Global dynamics of an HBV-HIV co-infection model incorporating latent reservoirs

Ahmed Elaiw[1,*], Abdulaziz Alhmadi[1,2,*], Aatef Hobiny[1,*]

[1] Department of Mathematics, Faculty of Science, King Abdulaziz University, Jeddah 21589, Saudi Arabia

[2] General Studies Department, Technical College, Technical and Vocational Training Corporation, Jeddah 21494, Saudi Arabia

*** Corresponding author:** Ahmed Elaiw, aelaiwksu.edu.sa@kau.edu.sa; Abdulaziz Alhmadi, ealhmadi@stu.kau.edu.sa; Aatef Hobiny, ahobany@kau.edu.sa

CITATION

Elaiw A, Alhmadi A, Hobiny A. Global dynamics of an HBV-HIV co-infection model incorporating latent reservoirs. Advances in Differential Equations and Control Processes. 2025; 32(2): 2873. https://doi.org/10.59400/adecp2873

ARTICLE INFO

Received: 27 February 2025
Accepted: 18 April 2025
Available online: 5 June 2025

Abstract: HBV and HIV are both blood-borne viruses with overlapping transmission routes, leading to higher HBV prevalence among people with HIV. While mathematical models have been extensively used to study each virus individually, co-infection dynamics have been relatively underexplored in research. This study presents a new within-host co-infection model for HIV and HBV that includes latent reservoirs. It accounts for HIV infecting both $CD4^+$ T cells and hepatocytes, while HBV targets only hepatocytes. The model features both latent and active infection states for each cell type, along with free viral particles for both viruses. The model undergoes a qualitative analysis, leading to the derivation of four threshold parameters ($\mathcal{R}_i$, $i = 0, 1, 2, 3$) that govern the existence and stability of its four equilibrium points. The stability conditions for each equilibrium of the model are determined through the construction of Lyapunov functions. Computational simulations are performed to confirm the key theoretical findings, while sensitivity analysis assesses how various parameters influence the basic reproductive numbers for HIV ($\mathcal{R}_0$) and HBV ($\mathcal{R}_1$) single-infections. The impact of anti-HIV and anti-HBV drugs is examined, and the critical efficacy thresholds for both therapies are identified. If the treatment effectiveness exceeds these thresholds, complete eradication of both HIV and HBV can be achieved.

Keywords: HIV; HBV; co-infection; global dynamics; Lyapunov stability
MSC: 34D20; 34D23; 37N25; 92B05

1. Introduction

Hepatitis B virus (HBV) and human immunodeficiency virus (HIV) are both major viral infections that impact the human body, each contributing to serious health complications. HIV is an RNA virus that primarily attacks $CD4^+$ T cells, which play a vital role in the adaptive immune response. In a healthy individual, $CD4^+$ T cell levels are usually around 1000 cells per mm^3. However, HIV infection gradually depletes these cells over time. When the $CD4^+$ T cell count drops below 200 cells per mm^3, the condition progresses to acquired immunodeficiency syndrome (AIDS) [1]. People with AIDS are more vulnerable to opportunistic infections and cancers as their immune system weakens, making it difficult for the body to defend against these diseases. In addition to targeting $CD4^+$ T cells, HIV can infect other immune cells such as dendritic cells and macrophages. The virus also has the ability to infect different liver cells, including hepatocytes, Kupffer cells, and infiltrating T cells [2,3]. HIV spreads through the bodily fluids of an infected person, including blood, semen, and vaginal fluids. HIV

remains a significant global health issue. As reported by UNAIDS, in 2023, there were 630,000 deaths due to HIV-related diseases, 1.3 million new infections, and a total of 39.9 million people living with the virus worldwide [4].

HBV is a DNA virus with a double-stranded structure that primarily targets liver cells (hepatocytes), resulting in inflammation and possible long-term health issues [5]. In some individuals, HBV infection can lead to chronic hepatitis and ongoing liver damage. As the infection persists, it raises the likelihood of developing liver fibrosis and cirrhosis over time [6]. HBV is commonly transmitted from mother to child during childbirth, in early childhood, and through contact with blood or other bodily fluids, such as during unprotected sex, unsterile injections, or exposure to contaminated sharp objects [7]. Approximately 30%–40% of individuals with chronic hepatitis B-related liver inflammation go on to develop cirrhosis [8]. Around 25% of those with chronic HBV are at increased risk of liver cancer [9]. According to the World Health Organization (WHO), there were an estimated 1.2 million new HBV infections in 2022, with 254 million people living with chronic HBV worldwide. The same year, about 1.1 million deaths were attributed to HBV [7].

HBV is frequently observed in individuals with HIV due to their overlapping modes of transmission. Worldwide, approximately 8% to 10% of people diagnosed with HIV also suffer from chronic HBV co-infection [10]. The simultaneous presence of HIV and HBV presents a significant public health challenge, as their interaction exacerbates health issues and raises the likelihood of severe complications [11]. Individuals with both infections are at a higher risk of developing severe liver conditions, including cirrhosis, hepatocellular carcinoma, and end-stage liver disease [12]. Furthermore, individuals co-infected with HIV and HBV face an increased risk of liver-related mortality compared to those with HBV infection alone [13]. Corcorran and Kim [10] emphasize that HIV-HBV co-infection accelerates liver disease progression and significantly increases the risk of liver-related death. HIV infection also heightens vulnerability to HBV, contributing to greater liver-related complications, increased morbidity, and higher mortality rates. According to Hogan et al. [14], people co-infected with HIV and HBV face a substantially increased likelihood of long-term liver impairment.

Investigating the interactions among viruses, host cells, and immune responses through laboratory experiments can be expensive. Consequently, mathematical modeling has become a crucial approach for understanding viral dynamics and their interactions with target and immune cells. These models also offer valuable insights into how viral co-infections impact human health and help evaluate the efficacy of interventions such as vaccines and antiviral treatments [15]. The basic model for describing HIV dynamics by Nowak and Bangham [16] serves as a fundamental framework for modeling various viruses that infect the human body. This model of HIV dynamics represents the interactions among three compartments: uninfected $CD4^+$ T cells, HIV-infected cells, and free virus particles. Numerous extensions and refinements on this model have been developed to better capture the complexities of HIV infections. Researchers have incorporated additional biological factors, such as the role of immune responses [16–18]; time delays [18, 19]; drug therapy [20]; reaction-diffusion [21,

22], cell-to-cell transmission [18, 22]; and age structure [22]. These developments have broadened the model's applicability, offering a greater understanding of viral persistence, immune system evasion, and therapeutic approaches.

The basic model for describing HBV mono-infection has been introduced in [23] which contains three components: uninfected hepatocytes, infected hepatocytes and free HBV particles. Numerous studies on the dynamics of HBV infection have made extensive use of this model by including different factors such as: time delays [6,24,25]; cell-to-cell transmission [26, 27]; spatial diffusion [28]; age structure [29, 30]; drug therapy [31]; and immune responses [32–34] (see also the review paper [35]).

Mathematical models have been instrumental in epidemiology, offering crucial insights into infectious disease dynamics and guiding public health interventions. Several studies have examined the interplay between HIV-HBV co-infection across different populations (see, e.g., [11, 36–38]). Bowong et al. [36] proposed a detailed mathematical framework that integrates key epidemiological and biological factors of both infections. Endashaw and Mekonnen [37] investigated the effects of vaccination and treatment on the transmission dynamics of HBV and HIV, emphasizing the need for widespread implementation of these interventions to curb co-infection rates. Further expanding on this research, Endashaw et al. [38] refined the previous model to assess the role of mother-to-child transmission (MTCT) in disease spread. Their results suggested that lowering MTCT rates can significantly reduce infection prevalence and aid in controlling the dual epidemic. Ullah et al. [11] developed a fractional-order model based on empirical data from Taiwan (2000–2023). Their study demonstrated that enhancing HBV vaccination efforts not only reduces HBV prevalence but also decreases the risk of co-infection, underscoring the importance of immunization in public health strategies.

As previously discussed, numerous mathematical models have been developed to analyze the within host dynamics of HIV and HBV mono-infections. However, mathematical modeling of the within-host interactions between HIV and HBV have received limited attention in research, with [39] and [40] being the only known studies exploring this topic. These studies assumed that HBV primarily infects hepatocytes in the liver, while HIV was also considered capable of infecting hepatocytes alongside its primary target, $CD4^+$ T cells. Nampala et al. [39] developed a mathematical model to assess the effects of hepatotoxicity and antiretroviral therapy on HIV and HBV co-infection. Through numerical simulations, they examined both the therapeutic benefits and potential toxicity of existing treatment regimens, ultimately identifying an optimal strategy for managing co-infection. Their proposed approach aimed to enhance treatment effectiveness while minimizing harmful side effects. However, the mathematical analysis in [39] was limited to evaluating the model's boundedness and positivity, focusing solely on the uninfected equilibrium and its stability. In a subsequent study, [40] introduced a co-dynamic model incorporating a time delay to reflect the period between viral entry and replication. This study proposed an optimized treatment strategy by reducing both HBV and HIV viral loads while balancing treatment expenses and medication-induced side effects, leading to lower pathogen density. However, the model in [40] did not account for the population dynamics of uninfected

and HIV-infected $CD4^+$ T cells, instead assuming a constant rate of HIV production from infected $CD4^+$ T cells. To address this limitation, our proposed model explicitly incorporates the population dynamics of both uninfected and HIV-infected $CD4^+$ T cells, allowing for a more realistic representation of HIV replication within the host. This enhancement provides a deeper understanding of the infection process and its impact on host cellular populations over time.

Highly active antiretroviral therapy (HAART) is known to be an effective treatment for controlling HIV infection and inhibiting its replication. However, it is unable to completely eliminate HIV from the body. Latently infected $CD4^+$ T cells pose a significant challenge to the eradication of the virus. These cells can evade both immune detection and the effects of antiretroviral therapy [41]. For an extended period, latently infected $CD4^+$ T cells are considered viral reservoirs, remaining dormant until triggered to produce new HIV particles. Numerous HIV mono-infection models have been developed that account for latent infection in $CD4^+$ T cells (see, e.g., [42–44]). Similarly, several studies have explored HBV mono-infection models incorporating latent HBV-infected hepatocytes (see, e.g., [6, 24, 25, 35]). We noted that the models described in [39, 40] excluded latent HIV-infected $CD4^+$ T cells as well as latent HBV-infected hepatocytes. To overcome this limitation, our model includes both latent HIV-infected $CD4^+$ T cells and latent HBV-infected hepatocytes, offering a more comprehensive representation of the viral reservoirs and their role in the persistence and progression of co-infection within the host. This enhancement allows for a better understanding of the long-term dynamics of both infections.

Stability analysis is a fundamental tool in the study of within-host viral infection models, providing essential insights into the progression and control of infections over time. It helps determine whether the immune system and drug therapies will eliminate the virus, the infection will reach a chronic steady state, or the viral load will escalate uncontrollably. By analyzing the stability of equilibrium points, such as infection-free or infected equilibria, researchers can predict long-term outcomes of viral behavior within the host. This method is particularly important for understanding complex interactions between viruses and host cells, evaluating treatment strategies, and guiding the development of effective therapeutic interventions. In [39], only the uninfected equilibrium was determined, and its stability was analyzed.

In this study, we propose a within-host model for HIV-HBV co-infection that includes the population dynamics of latent HIV-infected $CD4^+$ T cells, latent HIV-infected hepatocytes as well as latent HBV-infected hepatocytes. We analyze the fundamental properties of the model's solutions. Furthermore, we calculate the equilibrium points of the model and evaluated its global stability with respect to a set of threshold parameters. To validate the qualitative findings, extensive numerical simulations are performed, providing important biological insights. Additionally, a sensitivity analysis is carried out to evaluate the impact of key parameters on the model.

The organization of this paper is as follows: Sections 2 and 3 present the development of the HIV-HBV co-infection model, examine the non-negativity and boundedness of the solutions, and derive the basic reproductive numbers alongside the analysis of equilibrium points. Section 4 is dedicated to investigating the global

stability of these equilibria. Section 5 includes numerical simulations that support and illustrate the theoretical results. Lastly, Section 6 offers a concluding summary of the main findings and outlines potential avenues for future research.

2. Model formulation

This part offers an in-depth description of the suggested model. The development is grounded on these key assumptions:

A1: The model represents ten distinct populations: Uninfected hepatocytes, $x_1(t)$, latent HIV-infected hepatocytes, $l_1(t)$, active HIV-infected hepatocytes, $y_1(t)$, latent HBV-infected hepatocytes, $l_2(t)$, active HBV-infected hepatocytes, $y_2(t)$, uninfected CD4$^+$ T cells, $x_2(t)$, latent HIV-infected CD4$^+$ T cells, $l_3(t)$, active HIV-infected CD4$^+$ T cells, $y_3(t)$, free HIV, $v_1(t)$, free HBV, $v_2(t)$, where, t is the time. The compartments $(x_1, l_1, y_1, l_2, y_2, x_2, l_3, y_3, v_1, v_2)$ experience death (or clearance) at rates $(d_1x_1, \mu_1 l_1, a_1 y_1, \mu_2 l_2, a_2 y_2, d_2 x_2, \mu_3 l_3, a_3 y_3, c_1 v_1, c_2 v_2)$, respectively. The interactions between HIV and HBV dynamics are depicted in the schematic diagram in **Figure 1**.

A2: HBV specifically infects uninfected hepatocytes in the liver, as noted by Nowak et al. [23], while HIV targets two types of cells: uninfected hepatocytes ([2,3]) and uninfected CD4$^+$ T cells ([23]). Upon entering the liver, HIV has a probability (p) of infecting a hepatocyte and a complementary probability of $1-p$ for infecting a CD4$^+$ T cell ([39]).

A3: Uninfected hepatocytes are recurred at a constant rate λ_1 and are susceptible to infection by both HIV and HBV, with infection occurring at rates $p\beta_1 x_1 v_1$ and $\beta_2 x_1 v_2$, respectively [39] as shown in Equation (1). These hepatocytes then transition to latent HIV-infected and latent HBV-infected states at rates $p\beta_1 x_1 v_1$ and $\beta_2 x_1 v_2$, respectively, as detailed in Equations (2) and (4).

A4: Uninfected CD4$^+$ T cells are recurred at a constant rate λ_2 and are susceptible to HIV infection at a rate of $(1-p)\beta_1 x_1 v_1$ [16, 39] as indicated in Equation (6). These cells then transition to latent HIV-infected CD4$^+$ T cells at rate $(1-p)\beta_1 x_1 v_1$ [39] as indicated in Equation (7).

A5: HIV virions are released from two sources, active HIV-infected hepatocytes and active HIV-infected CD4$^+$ T cells at rates $k_1 a_1 y_1$ and $k_3 a_3 y_3$, respectively [16, 39] as shown in Equation (9, while HBV virions are released from active HBV-infected hepatocytes at a rate $of k_2 a_2 y_2$ [23, 39] as described in Equation (10).

Building on Assumptions A1–A5, we construct a co-infection model for HIV and HBV, represented as a system of ten ordinary differential equations (ODEs):

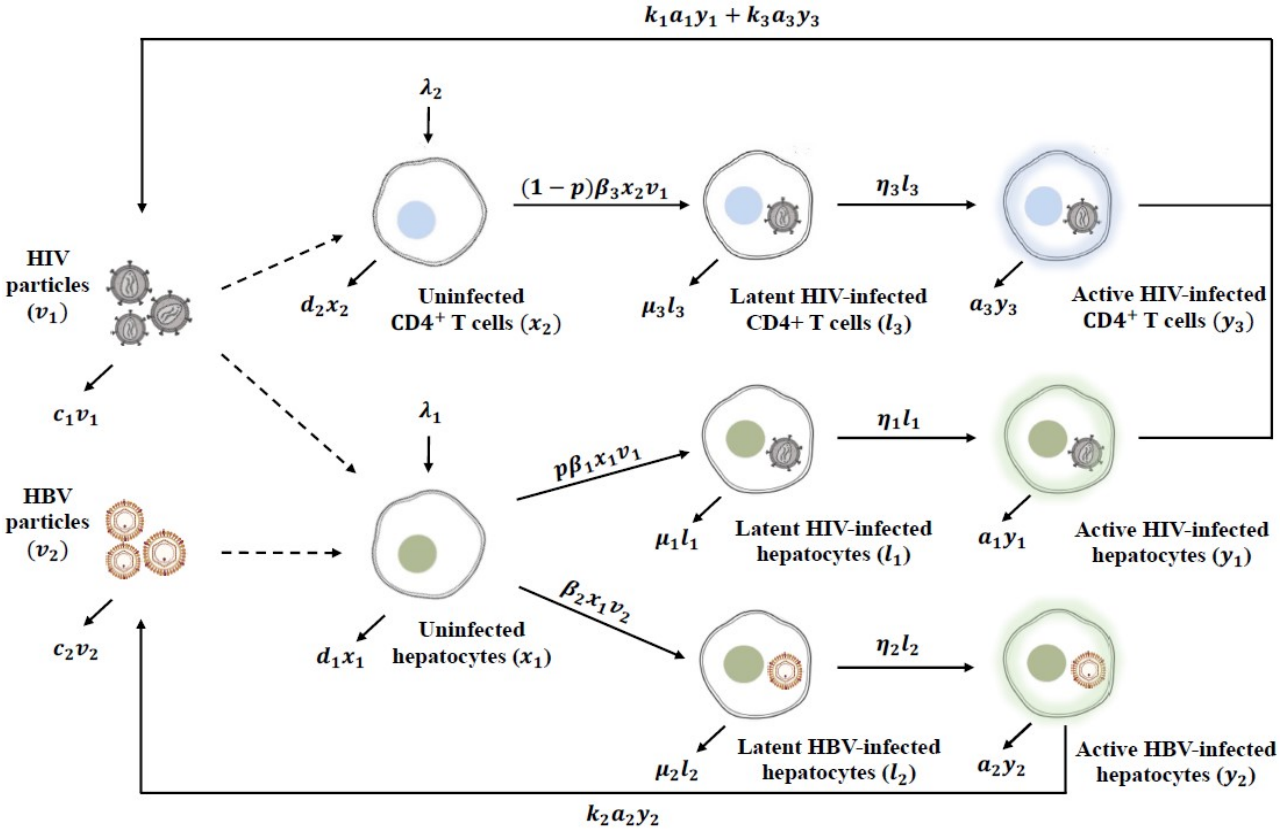

Figure 1. Schematic diagram for an HIV/HBV co-infection dynamics.

$$\dot{x}_1 = \lambda_1 - d_1x_1 - p\beta_1x_1v_1 - \beta_2x_1v_2 \tag{1}$$
$$\dot{l}_1 = p\beta_1x_1v_1 - (\mu_1 + \eta_1)l_1 \tag{2}$$
$$\dot{y}_1 = \eta_1l_1 - a_1y_1 \tag{3}$$
$$\dot{l}_2 = \beta_2x_1v_2 - (\mu_2 + \eta_2)l_2 \tag{4}$$
$$\dot{y}_2 = \eta_2l_2 - a_2y_2 \tag{5}$$
$$\dot{x}_2 = \lambda_2 - d_2x_2 - (1-p)\beta_3x_2v_1 \tag{6}$$
$$\dot{l}_3 = (1-p)\beta_3x_2v_1 - (\mu_3 + \eta_3)l_3 \tag{7}$$
$$\dot{y}_3 = \eta_3l_3 - a_3y_3 \tag{8}$$
$$\dot{v}_1 = k_1a_1y_1 + k_3a_3y_3 - c_1v_1 \tag{9}$$
$$\dot{v}_2 = k_2a_2y_2 - c_2v_2. \tag{10}$$

The parameter definitions are provided in **Table 1**.

3. Preliminaries

3.1. Biological feasible domain

To ensure the biological relevance of the model (1)–(10), it is crucial to verify that all state variables remain non-negative for $t \geq 0$. This means that if the initial conditions of the system are non-negative, the solutions will also stay non-negative for all $t \geq 0$. By demonstrating that the solutions are both bounded and non-negative, we validate the well-posedness of the model.

Table 1. Variables and parameters description.

Variable	**Description**
x_1	Uninfected hepatocytes
l_1	Latent HIV-infected hepatocytes
y_1	Active HIV-infected hepatocytes
l_2	Latent HBV-infected hepatocytes
y_2	Active HBV-infected hepatocytes
x_2	Uninfected CD4$^+$ T cells
l_3	Latent HIV-infected CD4$^+$ T cells
y_3	Active HIV-infected CD4$^+$ T cells
v_1	Free HIV
v_2	Free HBV
Parameter	**Description**
λ_1	Generation rate of uninfected hepatocytes, x_1
λ_2	Generation rate of uninfected CD4$^+$ T cells, x_2
β_1	Incidence rate between HIV and uninfected hepatocytes (v_1 and x_1)
β_2	Incidence rate between HBV and uninfected hepatocytes (v_2 and x_1)
β_3	Incidence rate between HIV and uninfected CD4$^+$ T cells (v_1 and x_2)
d_1	Mortality rate of uninfected hepatocytes
d_2	Mortality rate of uninfected CD4$^+$ T cells
a_1	Mortality rate of active HIV-infected hepatocytes
a_2	Mortality rate of active HBV-infected hepatocytes
a_3	Mortality rate of active HIV-infected CD4$^+$ T cells
μ_1	Mortality rate of latent HIV-infected hepatocytes
μ_2	Mortality rate of latent HBV-infected hepatocytes
μ_3	Mortality rate of latent HIV-infected CD4$^+$ T cells
η_1	Conversion rate from latent to active HIV-infected hepatocytes
η_2	Conversion rate from latent to active HBV-infected hepatocytes
η_3	Conversion rate from latent to active HIV-infected CD4$^+$ T cells
c_1	Destruction rate of free HIV
c_2	Destruction rate of free HBV
p	Probability that HIV particles infect hepatocytes
$k_i, i = 1, 2, 3$	The average number of viral particles released by one infected cell during its lifespan

Let $\sigma_1 = \min(d_1, \mu_1, a_1, \mu_2, a_2)$ and $\sigma_2 = \min(d_2, \mu_3, a_3)$. Let us define the feasible set for the model's variables, denoted by Ξ.

Lemma 1. *The dynamics* (1)–(10) *admits a positively invariant set*

$$\Xi = \left\{(x_1, l_1, y_1, l_2, y_2, x_2, l_3, y_3, v_1, v_2) \in \mathbb{R}^{10}_+;\ x_1 + l_1 + y_1 + l_2 + y_2 \leq \frac{\lambda_1}{\sigma_1},\ x_2 + l_3 + y_3 \leq \frac{\lambda_2}{\sigma_2}\right.$$
$$\left. v_1 \leq \frac{\lambda_1 k_1 a_1}{c_1 \sigma_1} + \frac{\lambda_2 k_3 a_3}{c_1 \sigma_2},\ v_2 \leq \frac{\lambda_1 k_2 a_2}{c_2 \sigma_1}\right\}.$$

Proof. Since we have

$$\begin{aligned}
&\dot{x}_1 \mid_{x_1=0} = \lambda_1 > 0\\
&\dot{l}_1 \mid_{l_1=0} = p\beta_1 x_1 v_1 \geq 0, \text{ for all } x_1, v_1 \geq 0\\
&\dot{y}_1 \mid_{y_1=0} = \eta_1 l_1 \geq 0, \text{ for all } l_1 \geq 0\\
&\dot{l}_2 \mid_{l_2=0} = \beta_2 x_1 v_2 \geq 0, \text{ for all } x_1, v_2 \geq 0\\
&\dot{y}_2 \mid_{y_2=0} = \eta_2 l_2 \geq 0, \text{ for all } l_2 \geq 0\\
&\dot{x}_2 \mid_{x_2=0} = \lambda_2 > 0\\
&\dot{l}_3 \mid_{l_3=0} = (1-p)\beta_3 x_2 v_1 \geq 0, \text{ for all } x_2, v_1 \geq 0\\
&\dot{y}_3 \mid_{y_3=0} = \eta_3 l_3 \geq 0, \text{ for all } l_3 \geq 0\\
&\dot{v}_1 \mid_{v_1=0} = k_1 a_1 y_1 + k_3 a_3 y_3 \geq 0, \text{ for all } y_1, y_3 \geq 0\\
&\dot{v}_2 \mid_{v_2=0} = k_2 a_2 y_2 \geq 0, \text{ for all } y_2 \geq 0.
\end{aligned}$$

Therefore, $\mathbb{R}^{10}_{\geq 0}$ is invariant by the model (1)–(10). Let us denote by $T_1 = x_1 + l_1 + y_1 + l_2 + y_2$ and $T_2 = x_2 + l_3 + y_3$ to be the sizes of the total hepatocytes and CD4$^+$ T cells compartments, respectively. From system (1)–(10) we have

$$\begin{aligned}
\dot{T}_1 &= \lambda_1 - d_1 x_1 - \mu_1 l_1 - a_1 y_1 - \mu_2 l_2 - a_2 y_2\\
&\leq \lambda_1 - \sigma_1 T_1 \Rightarrow T_1(t) \leq \frac{\lambda_1}{\sigma_1} \text{ if } T_1(0) \leq \frac{\lambda_1}{\sigma_1}.
\end{aligned}$$

Similarly,

$$\begin{aligned}
\dot{T}_2 &= \lambda_2 - d_2 x_2 - \mu_3 l_3 - a_3 y_3\\
&\leq \lambda_2 - \sigma_2 T_2 \Rightarrow T_2(t) \leq \frac{\lambda_2}{\sigma_2} \text{ if } T_2(0) \leq \frac{\lambda_2}{\sigma_2}.
\end{aligned}$$

From Equations (9)–(10) we have

$$\begin{aligned}
\dot{v}_1 &= k_1 a_1 y_1 + k_3 a_3 y_3 - c_1 v_1 \leq k_1 a_1 \frac{\lambda_1}{\sigma_1} + k_3 a_3 \frac{\lambda_2}{\sigma_2} - c_1 v_1\\
&\Rightarrow v_1(t) \leq \frac{\lambda_1 k_1 a_1}{c_1 \sigma_1} + \frac{\lambda_2 k_3 a_3}{c_1 \sigma_2} \text{ if } v_1(0) \leq \frac{\lambda_1 k_1 a_1}{c_1 \sigma_1} + \frac{\lambda_2 k_3 a_3}{c_1 \sigma_2},
\end{aligned}$$

and

$$\begin{aligned}
\dot{v}_2 &= k_2 a_2 y_2 - c_2 v_2 \leq \frac{\lambda_1 k_2 a_2}{\sigma_1} - c_2 v_2\\
&\Rightarrow v_2(t) \leq \frac{\lambda_1 k_2 a_2}{c_2 \sigma_1} \text{ if } v_2(0) \leq \frac{\lambda_1 k_2 a_2}{c_2 \sigma_1}.
\end{aligned}$$

Hence, Ξ is positively invariant w.r.t. system (1)–(10).□

Now, let us examine the existence of equilibrium points for the system.

3.2. Existence of equilibria

In this part, we study the existence of equilibria of model (1)–(7). To evaluate the basic reproductive number $\mathcal{R}_{Co}$ for the HBV and HIV co-infection model described by Equations (1)–(7), we apply the next-generation matrix method as outlined by [45] (see

Appendix A). The resulting expression for $\mathcal{R}_{Co}$ is:

$$\mathcal{R}_{Co} = \max\{\mathcal{R}_0, \mathcal{R}_1\}$$

where, $\mathcal{R}_0 = \mathcal{R}_{01} + \mathcal{R}_{02}$, and

$$\begin{aligned}
\mathcal{R}_{01} &= \frac{k_1 p \beta_1 \lambda_1}{c_1 d_1} \frac{\eta_1}{\mu_1 + \eta_1} \\
\mathcal{R}_{02} &= \frac{k_3 (1-p) \beta_3 \lambda_2}{c_1 d_2} \frac{\eta_3}{\mu_3 + \eta_3} \\
\mathcal{R}_1 &= \frac{k_2 \beta_2 \lambda_1}{c_2 d_1} \frac{\eta_2}{\mu_2 + \eta_2}.
\end{aligned}$$

It is crucial to highlight that $\mathcal{R}_0$ denotes the basic reproductive number for HIV mono-infection, whereas $\mathcal{R}_1$ corresponds to the basic reproductive number for HBV mono-infection (see Appendix A). Define $x_1^0 = \dfrac{\lambda_1}{d_1}$, $x_2^0 = \dfrac{\lambda_2}{d_2}$ and

$$\begin{aligned}
\mathcal{R}_2 &= \frac{\lambda_2 k_2 \beta_2 k_3 (1-p) \beta_3 \eta_2 \eta_3 (\mu_1 + \eta_1)}{k_1 p \beta_1 c_2 d_2 \eta_1 (\mu_2 + \eta_2)(\mu_3 + \eta_3) \left(\dfrac{\mathcal{R}_1}{\mathcal{R}_{01}} - 1 \right)} \\
\mathcal{R}_3 &= \frac{d_1 (1-p) \beta_3}{p \beta_1 d_2} \left(\frac{\mathcal{R}_1 - 1}{\mathcal{R}_2 - 1} \right).
\end{aligned}$$

As a result, we can derive the following key conclusion about the existence of the equilibria for the system (1)–(10).

Lemma 2.

- *Model* (1)–(10) *admits an infection-free equilibrium denoted by*

$$\mathcal{E}_0 = \left(x_1^0, 0, 0, 0, 0, x_2^0, 0, 0, 0, 0 \right).$$

- *If* $\mathcal{R}_0 > 1$*, then model* (1)–(10) *admits an HIV mono-infection equilibrium denoted by*

$$\bar{\mathcal{E}} = \left(\bar{x}_1, \bar{l}_1, \bar{y}_1, 0, 0, \bar{x}_2, \bar{l}_3, \bar{y}_3, \bar{v}_1, 0 \right).$$

- *If* $\mathcal{R}_1 > 1$*, then model* (1)–(10) *admits an HBV mono-infection equilibrium denoted by*

$$\tilde{\mathcal{E}} = \left(\frac{c_2(\mu_2 + \eta_2)}{k_2 \beta_2 \eta_2}, 0, 0, \frac{c_2 d_1}{\eta_2 k_2 \beta_2}(\mathcal{R}_1 - 1), \frac{c_2 d_1}{a_2 k_2 \beta_2}(\mathcal{R}_1 - 1), x_2^0, 0, 0, 0, \frac{d_1}{\beta_2}(\mathcal{R}_1 - 1) \right).$$

- *If* $\mathcal{R}_1 > \mathcal{R}_{01}$*,* $\mathcal{R}_2 > 1$*, and* $\mathcal{R}_3 > 1$ *then model* (1)–(7) *admits an HIV-HBV co-infection equilibrium denoted by* $\mathcal{E}^* = (x_1^*, l_1^*, y_1^*, l_2^*, y_2^*, x_2^*, l_3^*, y_3^*, v_1^*, v_2^*)$.

Proof. Equilibrium points are typically determined by setting all time derivatives to zero, which leads to the following:

$$\begin{cases} 0 = \lambda_1 - d_1 x_1 - p\beta_1 x_1 v_1 - \beta_2 x_1 v_2 \\ 0 = p\beta_1 x_1 v_1 - (\mu_1 + \eta_1) l_1 \\ 0 = \eta_1 l_1 - a_1 y_1 \\ 0 = \beta_2 x_1 v_2 - (\mu_2 + \eta_2) l_2 \\ 0 = \eta_2 l_2 - a_2 y_2 \\ 0 = \lambda_2 - d_2 x_2 - (1-p)\beta_3 x_2 v_1 \\ 0 = (1-p)\beta_3 x_2 v_1 - (\mu_3 + \eta_3) l_3 \\ 0 = \eta_3 l_3 - a_3 y_3 \\ 0 = k_1 a_1 y_1 + k_3 a_3 y_3 - c_1 v_1 \\ 0 = k_2 a_2 y_2 - c_2 v_2. \end{cases}$$

We have the following cases:

1. If $v_1 = v_2 = 0$, the model has infection-free equilibrium $\mathcal{E}_0 = \left(x_1^0, 0, 0, 0, 0, x_2^0, 0, 0, 0, 0\right)$.

2. If $v_1 \neq 0$ and $v_2 = 0$, we obtain

$$l_2 = y_2 = v_2 = 0, \quad x_1 = \frac{\lambda_1}{d_1 + p\beta_1 v_1}, \quad x_2 = \frac{\lambda_2}{d_2 + (1-p)\beta_3 v_1}, \quad l_1 = \frac{p\beta_1 \lambda_1 v_1}{(\mu_1 + \eta_1)(d_1 + p\beta_1 v_1)}$$
$$y_1 = \frac{\eta_1 p\beta_1 \lambda_1 v_1}{a_1(\mu_1 + \eta_1)(d_1 + p\beta_1 v_1)}, \quad l_3 = \frac{(1-p)\beta_3 \lambda_2 v_1}{(\mu_3 + \eta_3)(d_2 + (1-p)\beta_3 v_1)}$$
$$y_3 = \frac{\eta_3 (1-p)\beta_3 \lambda_2 v_1}{a_3(\mu_3 + \eta_3)(d_2 + (1-p)\beta_3 v_1)},$$

and v_1 satisfies the following equation

$$\frac{k_1 \eta_1 p\beta_1 \lambda_1}{(\mu_1 + \eta_1)(d_1 + p\beta_1 v_1)} + \frac{k_3 \eta_3 (1-p)\beta_3 \lambda_2}{(\mu_3 + \eta_3)(d_2 + (1-p)\beta_3 v_1)} - c_1 = 0.$$

Define a function f by

$$f(v_1) = \frac{k_1 \eta_1 p\beta_1 \lambda_1}{(\mu_1 + \eta_1)(d_1 + p\beta_1 v_1)} + \frac{k_3 \eta_3 (1-p)\beta_3 \lambda_2}{(\mu_3 + \eta_3)(d_2 + (1-p)\beta_3 v_1)} - c_1.$$

Then we have

$$\begin{aligned} f(0) &= \frac{k_1 \eta_1 p\beta_1 \lambda_1}{d_1(\mu_1 + \eta_1)} + \frac{k_3 \eta_3 (1-p)\beta_3 \lambda_2}{d_2(\mu_3 + \eta_3)} - c_1 \\ &= c_1 \left(\frac{k_1 \eta_1 p\beta_1 \lambda_1}{c_1 d_1(\mu_1 + \eta_1)} + \frac{k_3 \eta_3 (1-p)\beta_3 \lambda_2}{c_1 d_2(\mu_3 + \eta_3)} - 1 \right) \\ &= c_1 \left(\mathcal{R}_{01} + \mathcal{R}_{02} - 1 \right) \\ &= c_1 \left(\mathcal{R}_0 - 1 \right). \end{aligned}$$

Thus, $f(0) > 0$ when $\mathcal{R}_0 > 1$. We have $f(v_1) \to -c_1 < 0$ whenever $v_1 \to \infty$. Moreover,

$$f'(v_1) = -\left(\frac{k_1 \eta_1 p^2 \beta_1^2 \lambda_1}{(\mu_1 + \eta_1)(d_1 + p\beta_1 v_1)^2} + \frac{k_3 \eta_3 (1-p)^2 \beta_3^2 \lambda_2}{(\mu_3 + \eta_3)(d_2 + (1-p)\beta_3 v_1)^2} \right) < 0.$$

Therefore, f is a strictly decreasing function of v_1 and when $\mathcal{R}_0 > 1$, there exists

a unique $\bar{v}_1 \in (0,\infty)$ such that $f(\bar{v}_1)=0$. Thus,

$$\bar{x}_1=\frac{\lambda_1}{d_1+p\beta_1\bar{v}_1}>0,\ \bar{x}_2=\frac{\lambda_2}{d_2+(1-p)\beta_3\bar{v}_1}>0,\ \bar{l}_1=\frac{p\beta_1\lambda_1\bar{v}_1}{(\mu_1+\eta_1)(d_1+p\beta_1\bar{v}_1)}>0$$
$$\bar{y}_1=\frac{\eta_1 p\beta_1\lambda_1\bar{v}_1}{a_1(\mu_1+\eta_1)(d_1+p\beta_1\bar{v}_1)}>0,\ \bar{l}_3=\frac{(1-p)\beta_3\lambda_2\bar{v}_1}{(\mu_3+\eta_3)(d_2+(1-p)\beta_3\bar{v}_1)}>0$$
$$\bar{y}_3=\frac{\eta_3(1-p)\beta_3\lambda_2\bar{v}_1}{a_3(\mu_3+\eta_3)(d_2+(1-p)\beta_3\bar{v}_1)}>0,$$

where $\bar{v}_1$ satisfies the following quadratic equation:

$$a\bar{v}_1^2+b\bar{v}_1+c=0 \tag{11}$$

where

$$\begin{aligned}a&=c_1p(1-p)\beta_1\beta_3(\mu_1+\eta_1)(\mu_3+\eta_3)>0\\ b&=c_1(d_2p\beta_1+d_1(1-p)\beta_3)(\eta_1+\mu_1)(\eta_3+\mu_3)\\&\quad-(1-p)p\beta_1\beta_3(k_3\eta_3\lambda_2(\eta_1+\mu_1)+k_1\eta_1\lambda_1(\eta_3+\mu_3))\\ c&=c_1d_1d_2(\mu_1+\eta_1)(\mu_3+\eta_3)\left(1-\mathcal{R}_0\right).\end{aligned}$$

Clearly, $c<0$ if $\mathcal{R}_0>1$. Equation (11) has a positive solution

$$\bar{v}_1=\frac{-b+\sqrt{b^2-4ac}}{2a}>0.$$

We obtain an HIV mono-infection equilibrium

$$\bar{\mathcal{E}}=\left(\bar{x}_1,\bar{l}_1,\bar{y}_1,0,0,\bar{x}_2,\bar{l}_3,\bar{y}_3,\bar{v}_1,0\right).$$

This implies that $\bar{\mathcal{E}}$ exists when $\mathcal{R}_0>1$.

3. If $v_1=0$ and $v_2\neq 0$, the model has an HBV mono-infection equilibrium

$$\begin{aligned}\tilde{\mathcal{E}}&=\left(\tilde{x}_1,0,0,\tilde{l}_2,\tilde{y}_2,\tilde{x}_2,0,0,0,\tilde{v}_2\right)\\&=\left(\frac{c_2(\mu_2+\eta_2)}{k_2\beta_2\eta_2},0,0,\frac{c_2d_1}{\eta_2k_2\beta_2}(\mathcal{R}_1-1),\frac{c_2d_1}{a_2k_2\beta_2}(\mathcal{R}_1-1),x_2^0,0,0,0,\frac{d_1}{\beta_2}(\mathcal{R}_1-1)\right).\end{aligned}$$

Clearly, $\tilde{\mathcal{E}}$ exists when $\mathcal{R}_1>1$.

4. If $v_1\neq 0$ and $v_2\neq 0$, the model has an HIV-HBV co-infection equilibrium point

$$\mathcal{E}^*=(x_1^*,l_1^*,y_1^*,l_2^*,y_2^*,x_2^*,l_3^*,y_3^*,v_1^*,v_2^*)$$

where

$$x_1^* = \frac{c_2(\mu_2+\eta_2)}{k_2\beta_2\eta_2}, l_1^* = \frac{c_2d_2(\mu_2+\eta_2)p\beta_1}{k_2\beta_2(1-p)\beta_3\eta_2(\mu_1+\eta_1)}(\mathcal{R}_2-1)$$
$$y_1^* = \frac{c_2d_2\eta_1(\mu_2+\eta_2)p\beta_1}{a_1k_2\beta_2(1-p)\beta_3\eta_2(\mu_1+\eta_1)}(\mathcal{R}_2-1), l_2^* = \frac{p\beta_1c_2d_2}{k_2\beta_2(1-p)\beta_3\eta_2}(\mathcal{R}_2-1)(\mathcal{R}_3-1)$$
$$y_2^* = \frac{p\beta_1c_2d_2}{a_2k_2\beta_2(1-p)\beta_3}(\mathcal{R}_2-1)(\mathcal{R}_3-1), x_2^* = \frac{k_1p\beta_1c_2\eta_1(\mu_2+\eta_2)(\mu_3+\eta_3)}{k_2\beta_2k_3(1-p)\beta_3\eta_2\eta_3(\mu_1+\eta_1)}\left(\frac{\mathcal{R}_1}{\mathcal{R}_{01}}-1\right)$$
$$l_3^* = \frac{k_1p\beta_1c_2d_2\eta_1(\mu_2+\eta_2)}{k_2\beta_2k_3(1-p)\beta_3\eta_2\eta_3(\mu_1+\eta_1)}\left(\frac{\mathcal{R}_1}{\mathcal{R}_{01}}-1\right)(\mathcal{R}_2-1)$$
$$y_3^* = \frac{k_1p\beta_1c_2d_2\eta_1(\mu_2+\eta_2)}{k_2\beta_2k_3(1-p)\beta_3a_3\eta_2(\mu_1+\eta_1)}\left(\frac{\mathcal{R}_1}{\mathcal{R}_{01}}-1\right)(\mathcal{R}_2-1)$$
$$v_1^* = \frac{d_2}{(1-p)\beta_3}(\mathcal{R}_2-1), v_2^* = \frac{p\beta_1d_2}{\beta_2(1-p)\beta_3}(\mathcal{R}_2-1)(\mathcal{R}_3-1).$$

Evidently, $\mathcal{E}^*$ exists when $\mathcal{R}_1 > \mathcal{R}_{01}$, $\mathcal{R}_2 > 1$, and $\mathcal{R}_3 > 1$. This equilibrium signifies the simultaneous presence of both HIV and HBV infections.□

4. Global stability

In this section, we apply the Lyapunov method to analyze the global asymptotic stability of all stable states within the model (1)–(10). The construction of Lyapunov functions follows the approach detailed in [46]. Let $\mathcal{F}$ denote the candidate Lyapunov function, and let Ω' represent the largest invariant subset of $\Omega = \left\{(x_1, y_1, y_2, x_2, z_1, v_1, v_2) : \frac{d\mathcal{F}}{dt} = 0\right\}$. We utilize the relationship between the arithmetic mean and the geometric mean as follows:

$$\frac{r_1+r_2+\cdots+r_n}{n} \geq \sqrt[n]{r_1r_2\cdots r_n}, \text{ for all } r_1, r_2, \cdots, r_n \geq 0. \tag{12}$$

The next result indicates that if the maximum value between the reproductive numbers of HIV ($\mathcal{R}_0$) and HBV ($\mathcal{R}_1$) does not exceed 1, both infections are expected to steadily decline and eventually disappear, independent of the initial viral load or infection stage. This implies that, under these conditions, the host cannot sustain either virus, leading to their eventual eradication.

Theorem 1. *The infection-free equilibrium $\mathcal{E}_0$ is GAS when $\mathcal{R}_{Co} \leq 1$. Moreover, $\mathcal{E}_0$ is unstable when $\mathcal{R}_{Co} > 1$.*

The next result shows that when $\mathcal{R}_0$ exceeds 1 and $\mathcal{R}_1$ remains less than or equal to $1 + \frac{p\beta_1\bar{v}_1}{d_1}$, HIV can establish a stable infection within the host, regardless of the initial viral load or stage of disease. In this case, HIV continues to replicate and persist, while HBV fails to spread efficiently, making co-infection unsustainable. Consequently, HIV dominates the infection dynamics, resulting in its persistence and the eventual clearance of HBV from the system.

Theorem 2. *If the HIV mono-infection equilibrium $\bar{\mathcal{E}}$ exists ($\mathcal{R}_0 > 1$) then it is GAS under the condition $\mathcal{R}_1 \leq 1 + \frac{p\beta_1\bar{v}_1}{d_1}$.*

The next analysis indicates that when $\mathcal{R}_1$ exceeds 1 and $\frac{\mathcal{R}_{01}}{\mathcal{R}_1} + \mathcal{R}_{02}$ is less than or equal to 1, HBV is capable of firmly establishing itself within the host, independent of the starting infection level or disease progression. In such a scenario, HBV continues to replicate and persist, while HIV lacks the capacity to spread efficiently, thereby

hindering the possibility of co-infection. As a consequence, HBV emerges as the prevailing virus, remaining in the system while HIV is gradually cleared.

Theorem 3. *If the HBV mono-infection equilibrium $\tilde{\mathcal{E}}$ exists (if $\mathcal{R}_1 > 1$) then it is GAS under the condition $\frac{\mathcal{R}_{01}}{\mathcal{R}_1} + \mathcal{R}_{02} \leq 1$.*

The following results demonstrate that when the conditions $\mathcal{R}_1 > \mathcal{R}_{01}$, $\mathcal{R}_2 > 1$ and $\mathcal{R}_3 > 1$ are met, the system consistently progresses toward a stable co-infection state involving both HBV and HIV, irrespective of the initial viral concentrations or the host's disease stage. In this regime, both viruses possess sufficient reproductive potential to sustain their presence within the host, allowing them to coexist and replicate efficiently over time. This implies that the host environment supports the persistence of both pathogens, leading to long-term co-infection dynamics where neither virus is cleared naturally.

Theorem 4. *If the HIV-HBV co-infection equilibrium $\mathcal{E}^*$ exists (if $\mathcal{R}_1 > \mathcal{R}_{01}$, $\mathcal{R}_2 > 1$ and $\mathcal{R}_3 > 1$) then it is GAS.*

A concise summary of the existence conditions and global stability criteria for the four equilibrium points is presented in **Table 2**.

Table 2. Sufficient conditions for existence and global stability of the four equilibrium points of system (1)–(10).

Equilibrium	**Existence conditions**	**Global stability conditions**
$\mathcal{E}_0 = \left(x_1^0, 0, 0, 0, 0, x_2^0, 0, 0, 0, 0\right)$	None	$\mathcal{R}_{Co} \leq 1$
$\bar{\mathcal{E}} = \left(\bar{x}_1, \bar{l}_1, \bar{y}_1, 0, 0, \bar{x}_2, \bar{l}_3, \bar{y}_3, \bar{v}_1, 0\right)$	$\mathcal{R}_0 > 1$	$\mathcal{R}_1 \leq 1 + \frac{p\beta_1\bar{v}_1}{d_1}$ and $\mathcal{R}_0 > 1$
$\tilde{\mathcal{E}} = \left(\tilde{x}_1, 0, 0, \tilde{l}_2, \tilde{y}_2, \tilde{x}_2, 0, 0, 0, \tilde{v}_2\right)$	$\mathcal{R}_1 > 1$	$\mathcal{R}_1 > 1$, $\frac{\mathcal{R}_{01}}{\mathcal{R}_1} + \mathcal{R}_{02} \leq 1$
$\mathcal{E}^* = (x_1^*, l_1^*, y_1^*, l_2^*, y_2^*, x_2^*, l_3^*, y_3^*, v_1^*, v_2^*)$	$\mathcal{R}_1 > \mathcal{R}_{01}, \mathcal{R}_2 > 1, \mathcal{R}_3 > 1$	$\mathcal{R}_1 > \mathcal{R}_{01}, \mathcal{R}_2 > 1, \mathcal{R}_3 > 1$

5. Numerical simulations

5.1. Stability of equilibria

We conducted numerical simulations based on the system of Equations (1)–(7), using a combination of parameter values. A portion of these values, listed in **Table 3**, were drawn from previously published studies. For the remaining parameters, reasonable estimates were made solely for illustrative computational purposes. This approach was necessary due to the current unavailability of precise clinical data, particularly for individuals co-infected with HIV and HBV. The difficulty in accessing such data-whether due to ethical restrictions, logistical constraints, or limited patient samples-poses a challenge to achieving accurate parameter estimation. Despite these limitations, the selected values provide a useful basis for exploring the model's qualitative behavior and lay the groundwork for future studies as more data become accessible. The initial value problem is solved numerically with MATLAB's ode45 solver. To confirm the theoretical findings from previous sections, we modify specific parameters that play a crucial role in determining threshold values and, in turn, affect stability dynamics.

Table 3. Model parameters.

Parameter	Value	Source	Parameter	Value	Source
λ_1	10	[47,48]	c_1	2.4	[19,53,54]
λ_2	10	[20,49]	c_2	0.67	[23,32,55]
d_1	0.01	[6,50]	k_2	12.5541	[56]
d_2	0.01	[20,49]	k_3	100	[20,57]
a_2	0.0693	[51]	a_1	0.5	Assumed
a_3	0.1	[52]	k_1	6	Assumed
μ_1	0.02	Assumed	η_1	0.01	Assumed
μ_2	0.01	[6,50]	η_2	0.05	Assumed
μ_3	0.02	[53]	η_3	0.01	[58]
p	0.3	[39]			

To validate the analytical findings from Section 4, we conduct simulations using various initial conditions. By selecting specific parameter values for the infection rates β_1, β_2 and β_3, we establish the following four scenarios:

Case 1: For $\beta_1 = 0.0003$, $\beta_2 = 0.00002$ and $\beta_3 = 0.00004$ and by using the parameters values given in **Table 3**, we obtain $\mathcal{R}_0 = 0.4639 < 1$ and $\mathcal{R}_1 = 0.3123 < 1$, and the infection-free equilibrium $\mathcal{E}_0 = (1000, 0, 0, 0, 0, 1000, 0, 0, 0, 0)$ is GAS (see **Figure 2**). The numerical results presented in **Figure 2** validate the theoretical conclusions of theorem 1, demonstrating that the solution of the system (1)–(10) approaches the equilibrium $\mathcal{E}_0$ for any initial conditions. In this scenario, the system dynamics lead to a return of uninfected hepatocytes and $CD4^+$ T cells to their baseline, pre-infection equilibrium levels. Concurrently, all other compartments–comprising infected cells, circulating virus particles, and latent viral reservoirs–gradually approach zero as time progresses. This results in the complete elimination of the infections, with both HIV and HBV being eradicated from the host. Such an outcome indicates the establishment of a stable, infection-free state, where the drug therapies may effectively controls and removes both viral pathogens, ensuring their full clearance from the body.

Case 2: For $\beta_1 = 0.007$, $\beta_2 = 0.00002$ and $\beta_3 = 0.0001$ and by using the parameters values given in **Table 3**, we obtain $\mathcal{R}_0 = 2.7222 > 1$ and $\mathcal{R}_1 = 0.3123 < 8.1464 = 1 + \frac{p\beta_1\bar{v}_1}{d_1}$. In **Figure 3**, the solution of the system (1)–(10) converges, for all initial conditions, to the equilibrium $\bar{\mathcal{E}} = (122.754, 292.415, 5.848, 0, 0, 807.615, 64.128, 6.413, 34.031, 0)$. The obtained numerical results provided in **Figure 3** confirm the theoretical findings in theorem 2. In this scenario, HIV remains the sole persistent infection, while the HBV infection is completely cleared from the host. Despite the initial co-infection, the dynamics of the system lead to the eradication of HBV, with all HBV-infected hepatocytes and HBV particles eventually diminishing to zero. The persistence of HIV in this case suggests that, under the given conditions, the immune system or drug therapies are unable to fully eliminate the HIV infection, while it successfully resolves the HBV infection. This outcome highlights the differential persistence of the two viruses in the co-infection environment, where HIV continues to replicate and maintain its presence within the host.

Case 3: For $\beta_1 = 0.006$, $\beta_2 = 0.0002$ and $\beta_3 = 0.00001$ and by using the parameters values given in **Table 3**, we obtain $\mathcal{R}_0 = 1.5972 > 1$, $\mathcal{R}_1 = 3.1229 > 1$ and $\mathcal{R}_{02} + \dfrac{\mathcal{R}_{01}}{\mathcal{R}_1} = 0.5775 < 1$. **Figure 4** demonstrates that, for all initial conditions, the solution of the system (1)–(10) converges to the equilibrium $\tilde{\mathcal{E}} = (320.214, 0, 0, 113.298, 81.744, 1000, 0, 0, 0, 106.146)$. This result, as shown in **Figure 4**, supports the conclusions of Theorem 3. In this case, HBV becomes the only persistent infection, while HIV is completely eradicated from the host. Despite the initial dual infection, the system's dynamics lead to the full clearance of HIV, with all HIV-infected CD4$^+$ T cells, HIV-infected hepatocytes and HIV particles gradually declining to zero. On the other hand, HBV persists, with infected hepatocytes and the associated viral load maintaining a stable presence in the host. This outcome suggests that, under the given conditions, the immune response and antiviral treatments are effective in eliminating HIV but are less successful in fully resolving HBV. It underscores the differing persistence dynamics between the two viruses in a co-infected environment, where HBV continues to replicate and establish a long-term infection, while HIV is cleared.

Case 4: For $\beta_1 = 0.00015$, $\beta_2 = 0.0002$ and $\beta_3 = 0.001$ and by using the parameters values given in **Table 3**, we obtain $\mathcal{R}_1 = 3.1229 > \mathcal{R}_{01} = 0.0375$, $\mathcal{R}_2 = 9.84 > 1$, $\mathcal{R}_3 = 3.735 > 1$. **Figure 5** illustrates that the solution of the system (1)–(10) converges to the equilibrium for all given initial conditions $\mathcal{E}^* = (320.214, 60.66, 1.213, 82.967, 59.861, 101.662, 299.459, 29.946, 126.291, 77.73)$, which means that $\mathcal{E}^*$ is GAS. The numerical results presented in **Figure 5** validate the theoretical conclusions established in theorem 4. In this scenario, both HIV and HBV continue to persist within the host. The system's dynamics lead to the maintenance of stable, chronic infections for both viruses, with each virus sustaining a certain level of replication. Infected hepatocytes and CD4$^+$ T cells persist, and viral particles for both HIV and HBV remain detectable in the bloodstream. The immune system, while actively responding to both infections, is unable to completely eliminate either virus, resulting in a long-term co-infection state. This outcome reflects the complex interplay between the two viruses, where the host's immune response and antiviral treatments struggle to fully suppress both infections simultaneously, allowing both HIV and HBV to maintain a presence in the body over time.

To further validate the model, we analyze the local stability of all nonnegative equilibrium points for cases 1–4. For each equilibrium point, we calculate the eigenvalues $X_i,\ i = 1, 2, \cdots, 10$ of the matrix J, as described by Equation (B7). An equilibrium point is considered locally stable if all eigenvalues satisfy the condition $\mathrm{Re}(X_i) < 0,\ i = 1, 2, \cdots, 10$. The contact rates β_1, β_2 and β_3 are those specified in cases 1–4. **Table 4** displays the nonnegative equilibrium points, the real parts of their eigenvalues, and the evaluation of whether each equilibrium point is locally asymptotically stable. We found that when an equilibrium point is GAS, the other equilibrium points are unstable.

Table 4. Analysis of local stability for nonnegative equilibria in cases 1–4.

Case	Equilibrium point	Re(X_i) for $i = 1, \cdots, 10$	Stability
Case 1	$\mathcal{E}_0 = (1000, 0, 0, 0, 0, 1000, 0, 0, 0, 0)$	$-0.01, -0.01, -2.4, -0.5, -0.01,$ $-0.11, -0.67, -0.1, -0.03, -0.03$	Stable
Case 2	$\mathcal{E}_0 = (1000, 0, 0, 0, 0, 1000, 0, 0, 0, 0)$	$-0.01, -0.01, -2.38, -0.57, 0.04,$ $-0.12, -0.67, -0.1, -0.03, -0.03$	Unstable
	$\bar{\mathcal{E}} = (122.76, 292.42, 5.85, 0, 0,$ $807.62, 64.13, 6.41, 34.03, 0)$	$-2.4, -0.51, -0.12, -0.03, -0.01$ $-0.01, -0.08, -0.67, -0.08, -0.05$	Stable
Case 3	$\mathcal{E}_0 = (1000, 0, 0, 0, 0, 1000, 0, 0, 0, 0)$	$-0.01, -0.01, -2.39, -0.56, 0.02,$ $-0.1, -0.64, -0.2, 0.05, -0.03$	Unstable
	$\bar{\mathcal{E}} = (602.02, 132.66, 2.65, 0, 0,$ $997.44, 0.9, 0.09, 3.67, 0)$	$-2.4, -0.54, -0.1, -0.03, -0.01,$ $-0.01, -0.01, -0.65, 0.02, -0.17$	Unstable
	$\tilde{\mathcal{E}} = (320.21, 0, 0, 113.3, 81.74,$ $1000, 0, 0, 0, 106.15)$	$-0.01, -2.4, -0.52, -0.66, -0.14,$ $-0.1, -0.01, -0.01, -0.01, -0.03$	Stable
Case 4	$\mathcal{E}_0 = (1000, 0, 0, 0, 0, 1000, 0, 0, 0, 0)$	$-0.01, -0.01, -2.39, -0.5, 0.11,$ $-0.25, -0.64, -0.03, 0.05, -0.2$	Unstable
	$\bar{\mathcal{E}} = (634.54, 121.82, 2.44, 0, 0,$ $100.41, 299.86, 29.99, 127.99, 0)$	$-2.4, -0.5, -0.16, -0.04, -0.04,$ $-0.02, -0.03, -0.65, -0.17, 0.02$	Unstable
	$\tilde{\mathcal{E}} = (320.21, 0, 0, 113.3, 81.74,$ $1000, 0, 0, 0, 106.15)$	$-0.01, -2.39, -0.5, -0.66, -0.25,$ $0.11, -0.14, -0.01, -0.01, -0.03$	Unstable
	$\mathcal{E}^* = (320.21, 60.66, 1.21, 82.967, 59.86,$ $101.662, 299.46, 29.95, 126.29, 77.73)$	$-2.4, -0.66, -0.5, -0.14, -0.16,$ $-0.01, -0.01, -0.03, -0.03, -0.03$	Stable

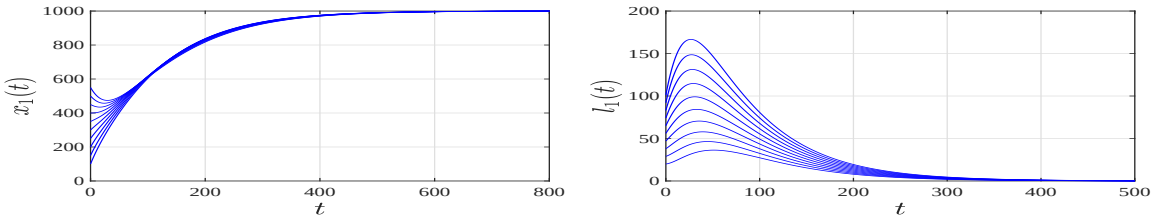

(a) Uninfected hepatocytes.

(b) Latent HIV-infected hepatocytes.

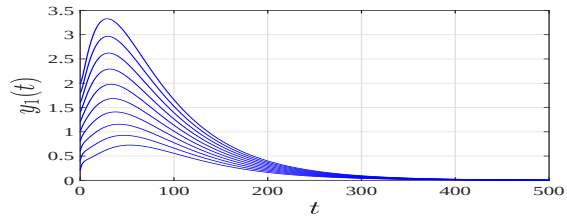

(c) Active HIV-infected hepatocytes.

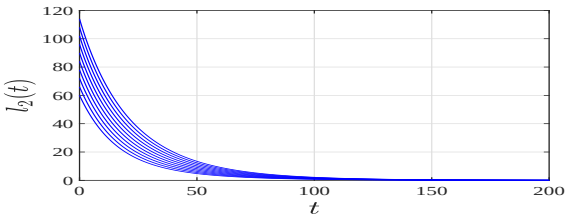

(d) Latent HBV-infected hepatocytes.

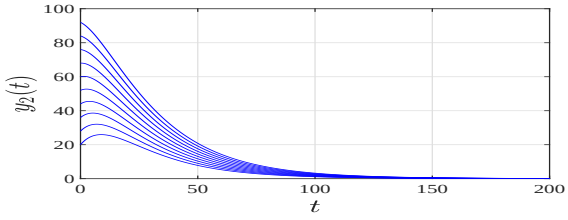

(e) Active HBV-infected hepatocytes.

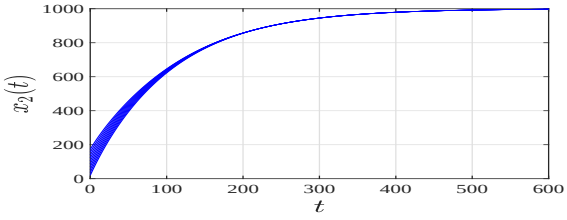

(f) Uninfected CD4$^+$ T cells.

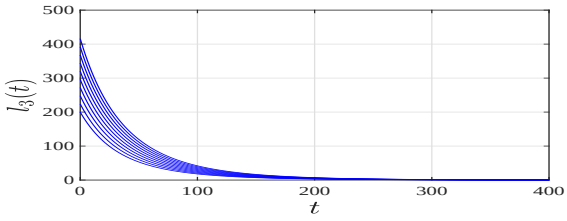

(g) Latent HIV-infected CD4$^+$ T cells.

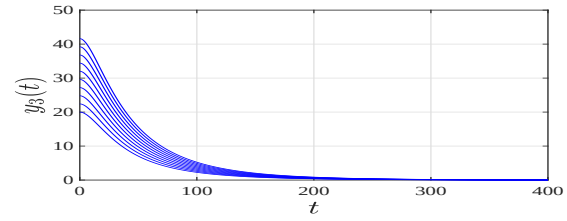

(h) Active HIV-infected CD4$^+$ T cells.

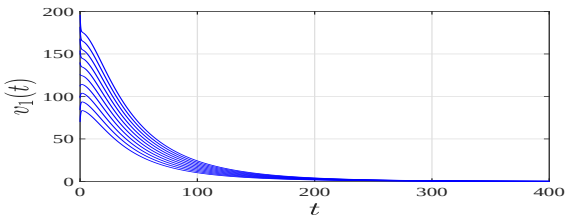

(i) Free HIV.

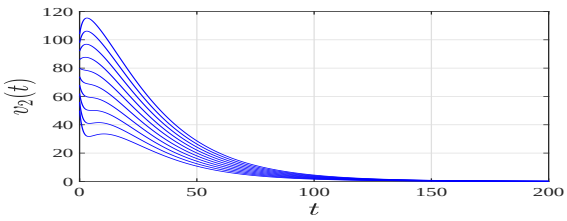

(j) Free HBV.

Figure 2. The solutions of system (1)–(10) with distinct initial states approach the equilibrium $\mathcal{E}_0 = (1000, 0, 0, 0, 0, 1000, 0, 0, 0, 0)$ reflecting the recovery from both HIV and HBV (case 1).

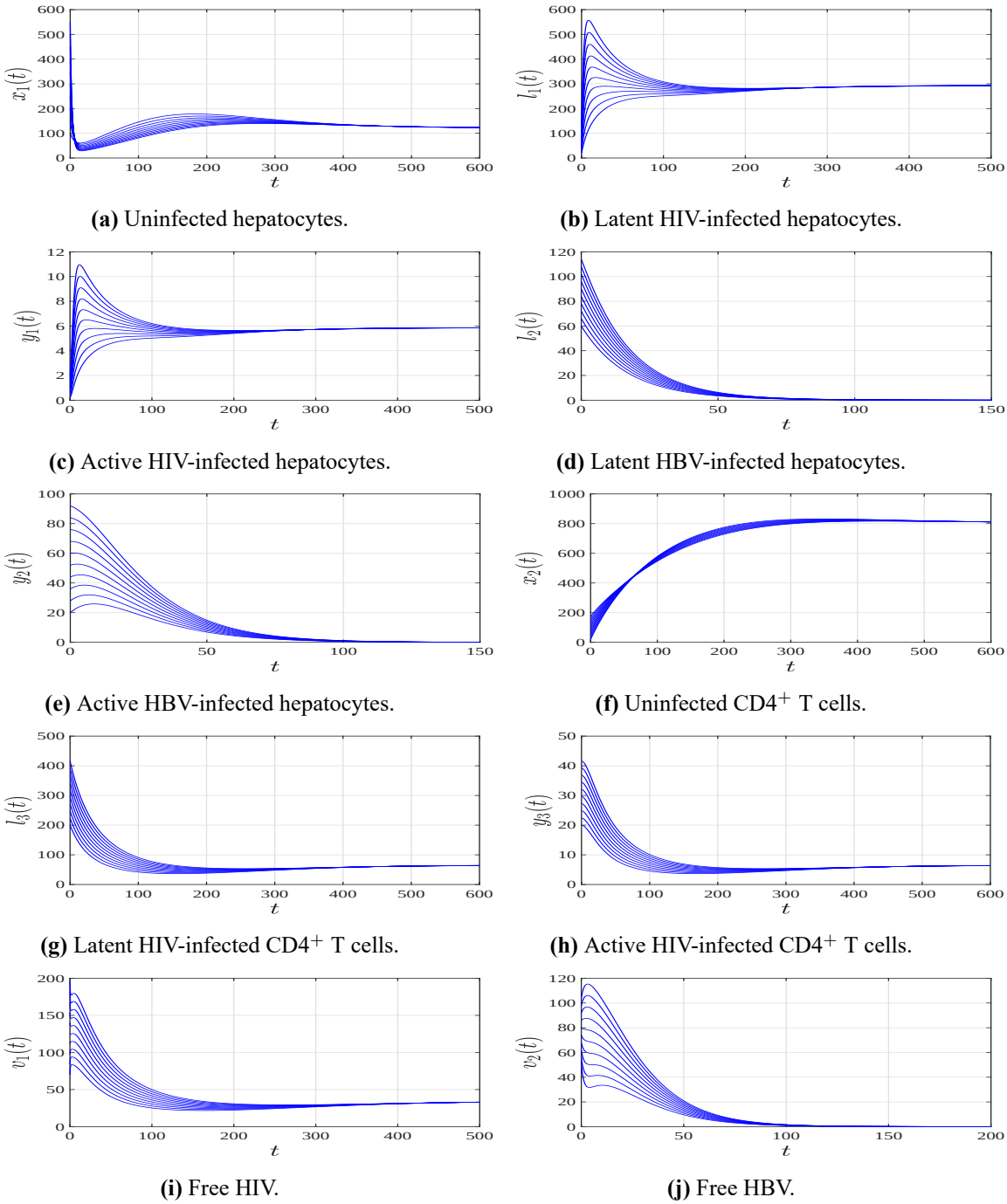

(a) Uninfected hepatocytes. **(b)** Latent HIV-infected hepatocytes.

(c) Active HIV-infected hepatocytes. **(d)** Latent HBV-infected hepatocytes.

(e) Active HBV-infected hepatocytes. **(f)** Uninfected CD4$^+$ T cells.

(g) Latent HIV-infected CD4$^+$ T cells. **(h)** Active HIV-infected CD4$^+$ T cells.

(i) Free HIV. **(j)** Free HBV.

Figure 3. The solutions of system (1)–(10) with distinct initial states approach the equilibrium $\bar{\mathcal{E}} = (122.754, 292.415, 5.848, 0, 0, 807.615, 64.128, 6.413, 34.031, 0)$ reflecting the persistence of the HIV single-infection (case 2).

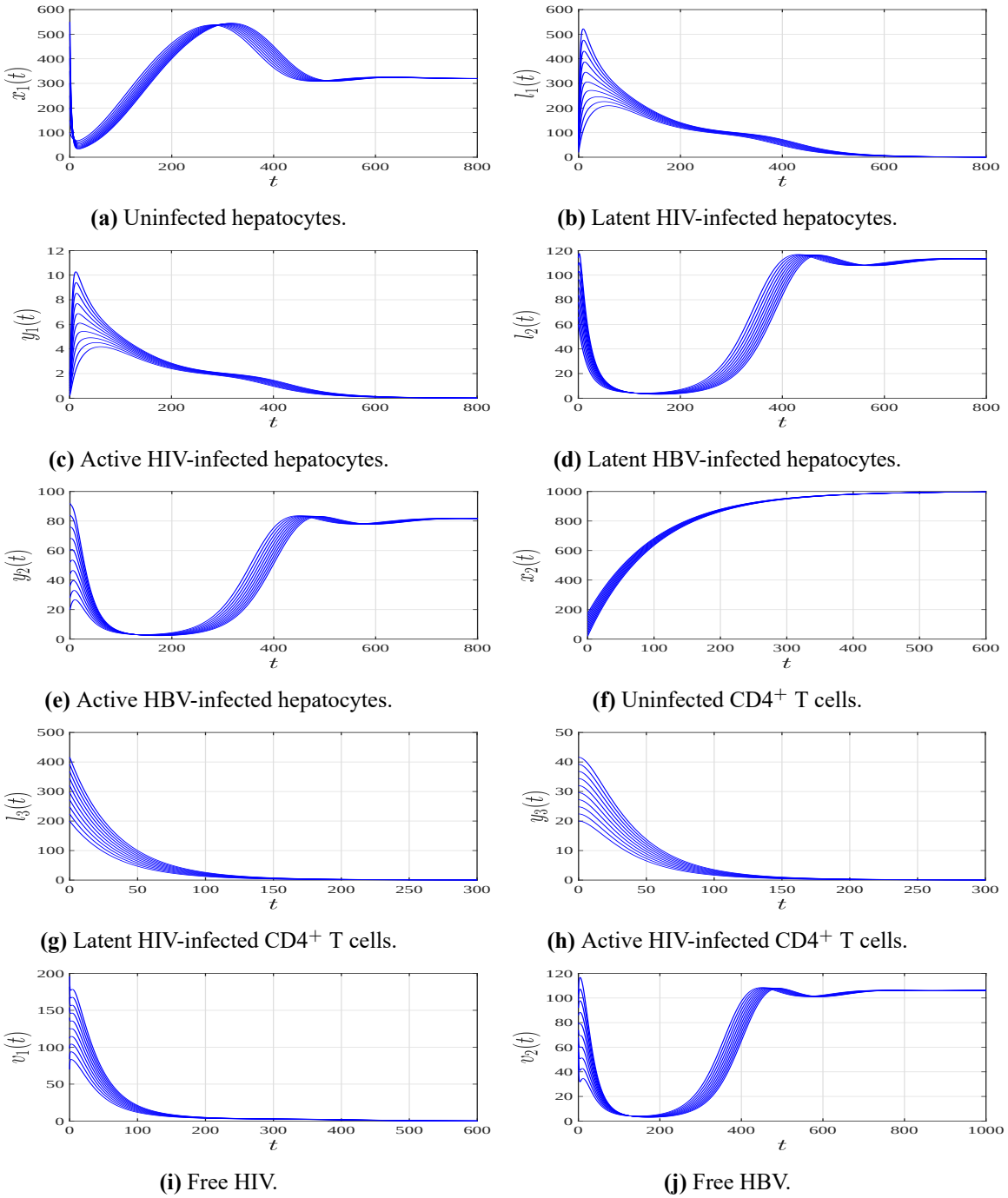

(a) Uninfected hepatocytes. **(b)** Latent HIV-infected hepatocytes.

(c) Active HIV-infected hepatocytes. **(d)** Latent HBV-infected hepatocytes.

(e) Active HBV-infected hepatocytes. **(f)** Uninfected CD4$^+$ T cells.

(g) Latent HIV-infected CD4$^+$ T cells. **(h)** Active HIV-infected CD4$^+$ T cells.

(i) Free HIV. **(j)** Free HBV.

Figure 4. The solutions of system (1)–(10) with distinct initial states approach the equilibrium $\tilde{\mathcal{E}} = (320.214, 0, 0, 113.298, 81.744, 1000, 0, 0, 0, 106.146)$ reflecting the persistence of the HBV single-infection (case 3).

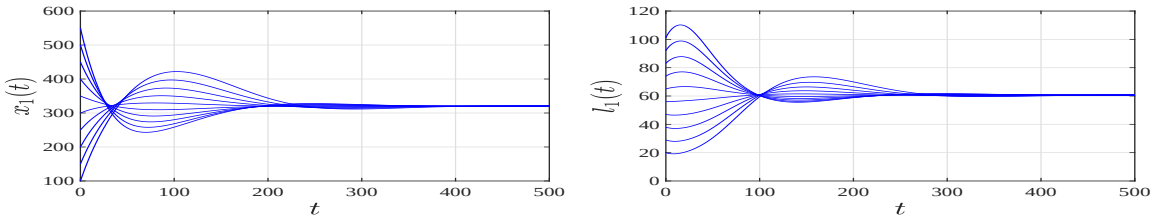

(a) Uninfected hepatocytes.

(b) Latent HIV-infected hepatocytes.

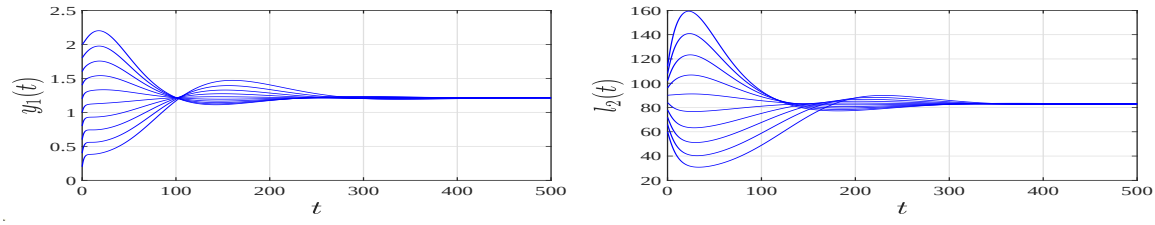

(c) Active HIV-infected hepatocytes.

(d) Latent HBV-infected hepatocytes.

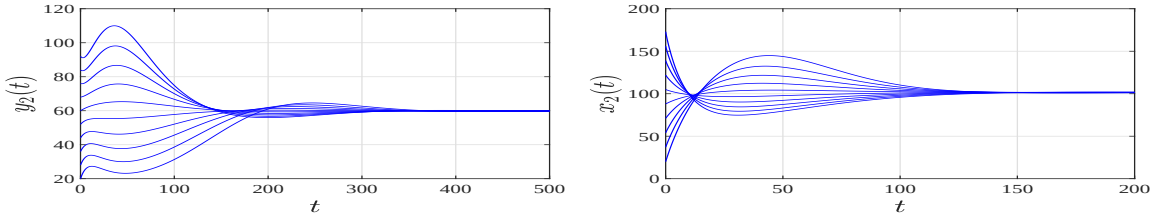

(e) Active HBV-infected hepatocytes.

(f) Uninfected CD4$^+$ T cells.

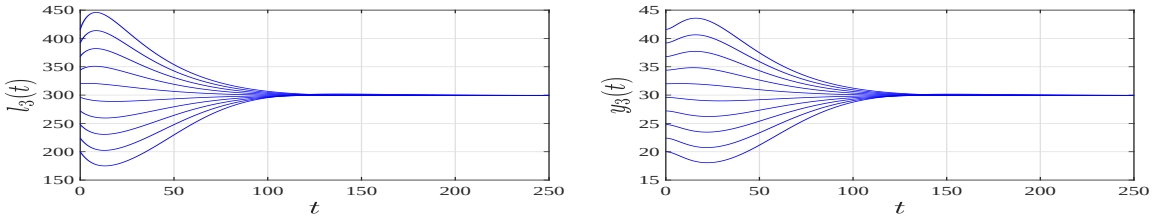

(g) Latent HIV-infected CD4$^+$ T cells.

(h) Active HIV-infected CD4$^+$ T cells.

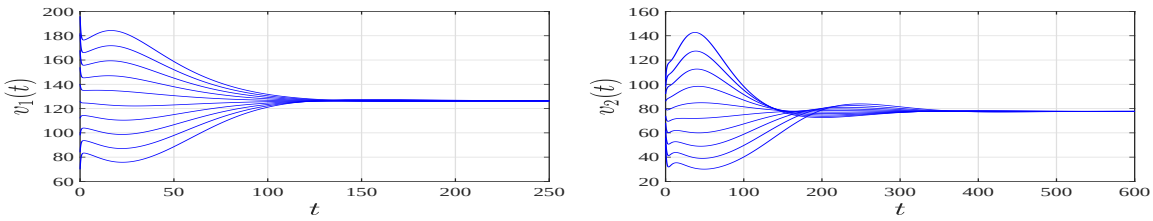

(i) Free HIV.

(j) Free HBV.

Figure 5. The solutions of system (1)–(10) with distinct initial states approach the equilibrium $\mathcal{E}^* = (320.214, 60.66, 1.213, 82.967, 59.861, 101.662, 299.459, 29.946, 126.291, 77.73)$ reflecting the persistence of both HIV and HBV infections (case 4).

5.2. Sensitivity analysis

Sensitivity analysis involves assessing and quantifying how input parameters affect the outcomes of a model. This is generally done using a sensitivity index, which quantifies the relative change in a variable as a result of changes in a parameter's value. This method helps pinpoint the parameters that have the most significant effect on the basic reproductive numbers $\mathcal{R}_0$ and $\mathcal{R}_1$. Given that $\mathcal{R}_0$ and $\mathcal{R}_1$ are differentiable with respect to certain parameters, sensitivity indices are derived using partial derivatives [59]. The goal of this analysis is to evaluate the sensitivity of both basic reproductive

numbers $\mathcal{R}_0$ and $\mathcal{R}_1$, and to assess their roles in determining the stability of the infection-free equilibrium $\mathcal{E}_0$. The sensitivity indices of $\mathcal{R}_0$ and $\mathcal{R}_1$ with respect to a parameter l are defined as:

$$S_l^{\mathcal{R}_i} = \frac{\partial \mathcal{R}_i}{\partial l} \times \frac{l}{\mathcal{R}_i}, i = 0, 1.$$

5.2.1. Sensitivity analysis for $\mathcal{R}_0$

The explicit expression of $\mathcal{R}_0$ is given by $\mathcal{R}_0 = \frac{k_1 p \beta_1 \lambda_1}{c_1 d_1} \frac{\eta_1}{\mu_1 + \eta_1} + \frac{k_3(1-p)\beta_3 \lambda_2}{c_1 d_2} \frac{\eta_3}{\mu_3 + \eta_3}$. Note that

$$S_{\lambda_1}^{\mathcal{R}_0} = S_{k_1}^{\mathcal{R}_0} = S_{\beta_1}^{\mathcal{R}_0} = -S_{d_1}^{\mathcal{R}_0} = \frac{\lambda_1 k_1 p \beta_1}{c_1 d_1 \mathcal{R}_0} \frac{\eta_1}{\mu_1 + \eta_1}, S_{\lambda_2}^{\mathcal{R}_0} = S_{k_3}^{\mathcal{R}_0} = S_{\beta_3}^{\mathcal{R}_0} = -S_{d_2}^{\mathcal{R}_0} = \frac{\lambda_2 k_3 (1-p)\beta_3}{c_1 d_2 \mathcal{R}_0} \frac{\eta_3}{\mu_3 + \eta_3}$$
$$S_{c_1}^{\mathcal{R}_0} = -1, S_p^{\mathcal{R}_0} = \frac{p}{\mathcal{R}_0} \left(\frac{k_1 \beta_1 \lambda_1}{c_1 d_1} \frac{\eta_1}{\mu_1 + \eta_1} - \frac{k_3 \beta_3 \lambda_2}{c_1 d_2} \frac{\eta_3}{\mu_3 + \eta_3} \right), S_{\eta_1}^{\mathcal{R}_0} = -S_{\mu_1}^{\mathcal{R}_0} = \frac{k_1 p \beta_1 \lambda_1}{\mathcal{R}_0 c_1 d_1} \frac{\eta_1 \mu_1}{(\mu_1 + \eta_1)^2}$$
$$S_{\eta_3}^{\mathcal{R}_0} = -S_{\mu_3}^{\mathcal{R}_0} = \frac{k_3(1-p)\beta_3 \lambda_2}{\mathcal{R}_0 c_1 d_2} \frac{\eta_3 \mu_3}{(\mu_3 + \eta_3)^2}.$$

Consider the parameter values $\beta_1 = 0.00015$, $\beta_2 = 0.0002$ and $\beta_3 = 0.001$. Based on the parameter values listed in **Table 3**, the sensitivity indices of $\mathcal{R}_0$ with respect to the model parameters are shown in **Table 5** and are depicted in **Figure 6**.

Table 5. Sensitivity of $\mathcal{R}_0$.

Parameter l	λ_1	k_1	β_1	λ_2	k_3	β_3	η_3
$S_l^{\mathcal{R}_0}$	0.0038	0.0038	0.0038	0.9962	0.9962	0.9962	0.6641
Parameter l	η_1	μ_1	d_1	p	μ_3	d_2	c_1
$S_l^{\mathcal{R}_0}$	0.0026	−0.0026	−0.0038	−0.4231	−0.6641	−0.9962	−1

The sensitivity indices of $\mathcal{R}_0$ with respect to λ_1, k_1, β_1, λ_2, k_3, β_3, η_1 and η_3 are positive, whereas, the indices of $\mathcal{R}_0$ with respect to μ_1, μ_3, d_1, d_2, p and c_1 are negative. Therefore, an increase of the values of parameters λ_1, k_1, β_1, λ_2, k_3, β_3, η_1 or η_3 results in a higher value of $\mathcal{R}_0$, however, an increase of the values of parameters μ_1, μ_3, d_1, d_2, p or c_1 results in a lower value of $\mathcal{R}_0$.

Based on the values in **Table 5**, a 100% increase (or decrease) in λ_1, k_1, or β_1 will lead to a 0.38% increase (or decrease) in the value of $\mathcal{R}_0$. Similarly, increasing (respectively, decreasing) λ_2, k_3, or β_3 by 100% will increase (or decrease) the $\mathcal{R}_0$ value by 99.62%. However, increasing (or decreasing) d_1 by 100% will decrease (respectively, increase) the $\mathcal{R}_0$ value by 0.38%. In the same way, a 100% increase (or decrease) in d_2 will result in a 99.62% decrease (or increase) in the value of $\mathcal{R}_0$. Same, a 100% increase (or decrease) in η_1 will result in a 0.26% increase (or decrease) in the value of $\mathcal{R}_0$, however, a 100% increase (or decrease) in μ_1 will result in a 0.26% decrease (or increase) in the value of $\mathcal{R}_0$. A 100% increase (or decrease) in η_3 will result in a 66.41% increase (or decrease) in the value of $\mathcal{R}_0$, however, a 100% increase (or decrease) in μ_3 will result in a 66.41% decrease (or increase) in the value of $\mathcal{R}_0$.

Similarly, increasing p by 100% will decrease the $\mathcal{R}_0$ value by 42.31%. Lastly, a 100% increase (or decrease) in c_1 will lead to a 100% decrease (or increase) in the value of $\mathcal{R}_0$. Note that $\mathcal{R}_0$ is not sensitive to the other parameters of system (1)–(10). We note that, $\mathcal{R}_0$ is most affected by the parameters λ_2, k_3, β_3, d_2 and c_1. This is consistent with biology, where HIV primarily targets CD4$^+$ T cells.

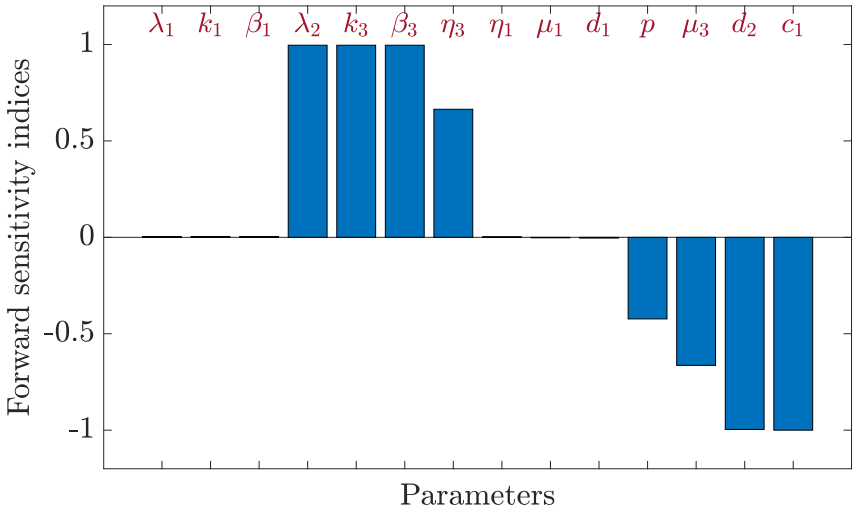

Figure 6. Sensitivity analysis for $\mathcal{R}_0$.

5.2.2. Sensitivity analysis for $\mathcal{R}_1$

The explicit expression of $\mathcal{R}_1$ is given by $\mathcal{R}_1 = \dfrac{k_2\beta_2\lambda_1}{c_2d_1}\dfrac{\eta_2}{\mu_2+\eta_2}$. Note that $S_{\eta_2}^{\mathcal{R}_1} = -S_{\mu_2}^{\mathcal{R}_1} = \dfrac{\mu_2}{\mu_2+\eta_2}$, $S_{\lambda_1}^{\mathcal{R}_1} = S_{k_2}^{\mathcal{R}_1} = S_{\beta_2}^{\mathcal{R}_1} = 1$ and $S_{d_1}^{\mathcal{R}_1} = S_{c_2}^{\mathcal{R}_1} = -1$. Let us select the parameter's values $\beta_1 = 0.00015$, $\beta_2 = 0.0002$ and $\beta_3 = 0.001$ and by using the parameters values given in **Table 3**, the sensitivity indices of $\mathcal{R}_1$ are given in **Table 6** and are depicted in **Figure 7**.

Table 6. Sensitivity of $\mathcal{R}_1$.

Parameter l	k_2	β_2	λ_1	η_2	μ_2	c_2	d_1
$S_l^{\mathcal{R}_1}$	1	1	1	0.1667	−0.1667	−1	−1

The indices of $\mathcal{R}_1$ with respect to k_2, β_2, λ_1 and η_2 are positive, whereas, the indices of $\mathcal{R}_1$ with respect to μ_2, c_2 and d_1 are negative. Therefore, an increase of the values of parameters k_2, β_2, λ_1 or η_2 causes an increase in the value of $\mathcal{R}_1$, whereas, increasing the values of parameters μ_2, c_2 or d_1 results in a decrease in the value of $\mathcal{R}_1$. For example, increasing (respectively, decreasing) k_2, β_2 or λ_1 by 100% will increase (or decrease) the $\mathcal{R}_1$ value by 100%. However, increasing (or decreasing) c_2 or d_1 by 100% will decrease (respectively, increase) the $\mathcal{R}_1$ value by 100%. Furthermore, increasing (or decreasing) η_2 by 100% will increase (respectively, decrease) the $\mathcal{R}_1$ value by 16.67%, however, increasing (or decreasing) μ_2 by 100% will decrease (respectively, increase) the $\mathcal{R}_1$ value by 16.67%. Note that $\mathcal{R}_1$ is not sensitive to the other parameters of system (1)–(10).

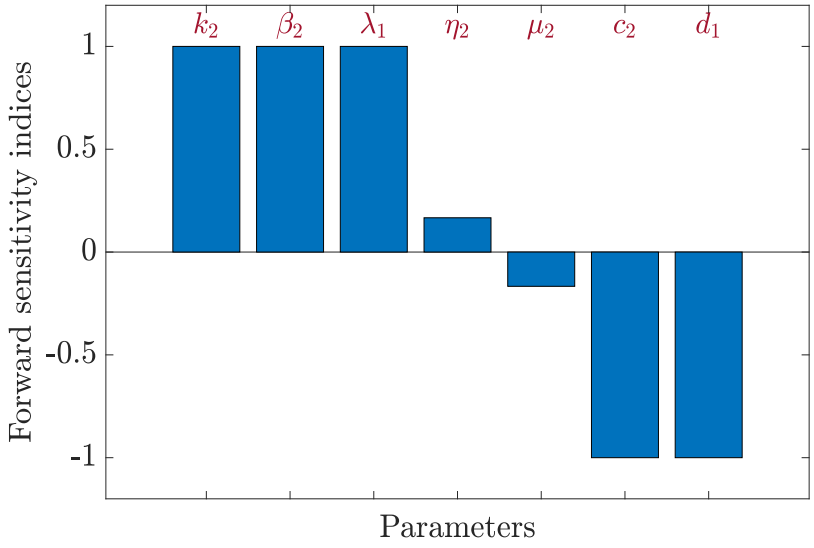

Figure 7. Sensitivity analysis for $\mathcal{R}_1$.

5.3. HIV-HBV co-infection under the influence of anti-HIV and anti-HBV therapies

To analyze the effect of antiviral treatments on the dynamics of HIV-HBV co-infection, we introduce a modified version of the system (1)–(10), incorporating two antiviral therapies aimed at inhibiting viral infections: (i) an Anti-HIV drug with efficacy $\epsilon_1 \in [0, 1]$ [20], and (ii) an Anti-HBV drug with efficacy $\epsilon_2 \in [0, 1]$ [60].

$$\dot{x}_1 = \lambda_1 - d_1 x_1 - p(1-\epsilon_1)\beta_1 x_1 v_1 - (1-\epsilon_2)\beta_2 x_1 v_2 \tag{13}$$
$$\dot{l}_1 = p(1-\epsilon_1)\beta_1 x_1 v_1 - (\mu_1 + \eta_1) l_1 \tag{14}$$
$$\dot{y}_1 = \eta_1 l_1 - a_1 y_1 \tag{15}$$
$$\dot{l}_2 = (1-\epsilon_2)\beta_2 x_1 v_2 - (\mu_2 + \eta_2) l_2 \tag{16}$$
$$\dot{y}_2 = \eta_2 l_2 - a_2 y_2 \tag{17}$$
$$\dot{x}_2 = \lambda_2 - d_2 x_2 - (1-\epsilon_1)(1-p)\beta_3 x_2 v_1 \tag{18}$$
$$\dot{l}_3 = (1-\epsilon_1)(1-p)\beta_3 x_2 v_1 - (\mu_3 + \eta_3) l_3 \tag{19}$$
$$\dot{y}_3 = \eta_3 l_3 - a_3 y_3 \tag{20}$$
$$\dot{v}_1 = k_1 a_1 y_1 + k_3 a_3 y_3 - c_1 v_1 \tag{21}$$
$$\dot{v}_2 = k_2 a_2 y_2 - c_2 v_2. \tag{22}$$

The basic reproductive numbers for model (13)–(22) are given as:

$$\mathcal{R}_0(\epsilon_1) = \frac{k_1(1-\epsilon_1)p\beta_1\lambda_1}{c_1 d_1}\frac{\eta_1}{\mu_1+\eta_1} + \frac{k_3(1-\epsilon_1)(1-p)\beta_3\lambda_2}{c_1 d_2}\frac{\eta_3}{\mu_3+\eta_3} = (1-\epsilon_1)\mathcal{R}_0(0) \leq \mathcal{R}_0(0)$$
$$\text{and } \mathcal{R}_1(\epsilon_2) = \frac{k_2(1-\epsilon_2)\beta_2\lambda_1}{c_2 d_1}\frac{\eta_2}{\mu_2+\eta_2} = (1-\epsilon_2)\mathcal{R}_1 \leq \mathcal{R}_1.$$

Assume that $\mathcal{R}_0(0) > 1$ and $\mathcal{R}_1(0) > 1$, with the goal of reducing $\mathcal{R}_0(\epsilon_1) \leq 1$ and $\mathcal{R}_1(\epsilon_2) \leq 1$, thereby stabilizing the system at the infection-free equilibrium $\mathcal{E}_0$. Let's calculate the threshold drug efficacies ϵ_1^{th} and ϵ_2^{th} as follows:

$$\mathcal{R}_0(\epsilon_1^{\text{th}}) = 1 \Rightarrow \epsilon_1^{\text{th}} = 1 - \frac{1}{\mathcal{R}_0(0)}$$
$$\mathcal{R}_1(\epsilon_2^{\text{th}}) = 1 \Rightarrow \epsilon_2^{\text{th}} = 1 - \frac{1}{\mathcal{R}_1(0)}.$$

Then we obtain

$$\mathcal{R}_0(\epsilon_1) \leq 1 \text{ for all } \epsilon_1^{\text{th}} \leq \epsilon_1 \leq 1$$
$$\mathcal{R}_1(\epsilon_2) \leq 1 \text{ for all } \epsilon_2^{\text{th}} \leq \epsilon_2 \leq 1$$

and thus $\mathcal{E}_0$ is GAS. This implies that both HIV and HBV will be eliminated.

Taking values $\beta_1 = 0.00015$, $\beta_2 = 0.0002$ and $\beta_3 = 0.001$ and the parameters values given in **Table 3**, we obtain $\epsilon_1^{\text{th}} = 0.8975$ and $\epsilon_2^{\text{th}} = 0.6798$, respectively. Consequently,

(i) if $0.8975 \leq \epsilon_1 \leq 1$ and $0.6798 \leq \epsilon_2 \leq 1$, then $\mathcal{R}_0(\epsilon_1) \leq 1$ and $\mathcal{R}_1(\epsilon_2) \leq 1$, and $\mathcal{E}_0$ is GAS;

(ii) if $0 \leq \epsilon_1 < 0.8975$ and/or $0 \leq \epsilon_2 < 0.6798$, then $\mathcal{R}_0(\epsilon_1) > 1$ and/or $\mathcal{R}_1(\epsilon_2) > 1$, and $\mathcal{E}_0$ will become unstable, and in this scenario, another equilibrium will emerge as GAS.

We now examine the dynamics of HIV-HBV co-infection under the influence of antiviral drug treatments. The system of Equations (13)–(22) is solved with the initial conditions

I.5: $(x_1(0), l_1(0), y_1(0), l_2(0), y_2(0), x_2(0), l_3(0), y_3(0), v_1(0), v_2(0)) = (750, 11, 0.2, 40, 25, 650, 150, 15, 45, 30)$.

We choose various values for the drug efficacies ϵ_1 and ϵ_2, as specified in **Table 7**.

Table 7. Variation of $\mathcal{R}_0(\epsilon_1)$ and $\mathcal{R}_1(\epsilon_2)$ with respect to the drug efficacies ϵ_1 and ϵ_2.

Cases	$\boldsymbol{\epsilon_1}$	$\boldsymbol{\epsilon_2}$	$\boldsymbol{\mathcal{R}_0(\epsilon_1)}$	$\boldsymbol{\mathcal{R}_1(\epsilon_2)}$
DE-1	0.7	0.4	2.9279	1.8738
DE-2	0.75	0.5	2.4399	1.5615
DE-3	0.8	0.6	1.9519	1.2492
DE-4	0.8975	0.6798	1	1
DE-5	0.95	0.75	0.488	0.7807

As shown in **Table 7** and **Figure 8**, enhancing the drug efficacies ϵ_1 and ϵ_2 results in a decrease in the reproductive numbers $\mathcal{R}_0(\epsilon_1)$ and $\mathcal{R}_1$, while simultaneously increasing the levels of uninfected hepatocytes and $CD4^+$ T cells. At the same time, the concentrations in other compartments decrease. This indicates that the use of anti-HIV and anti-HBV therapies contributes to improving the patient's health.

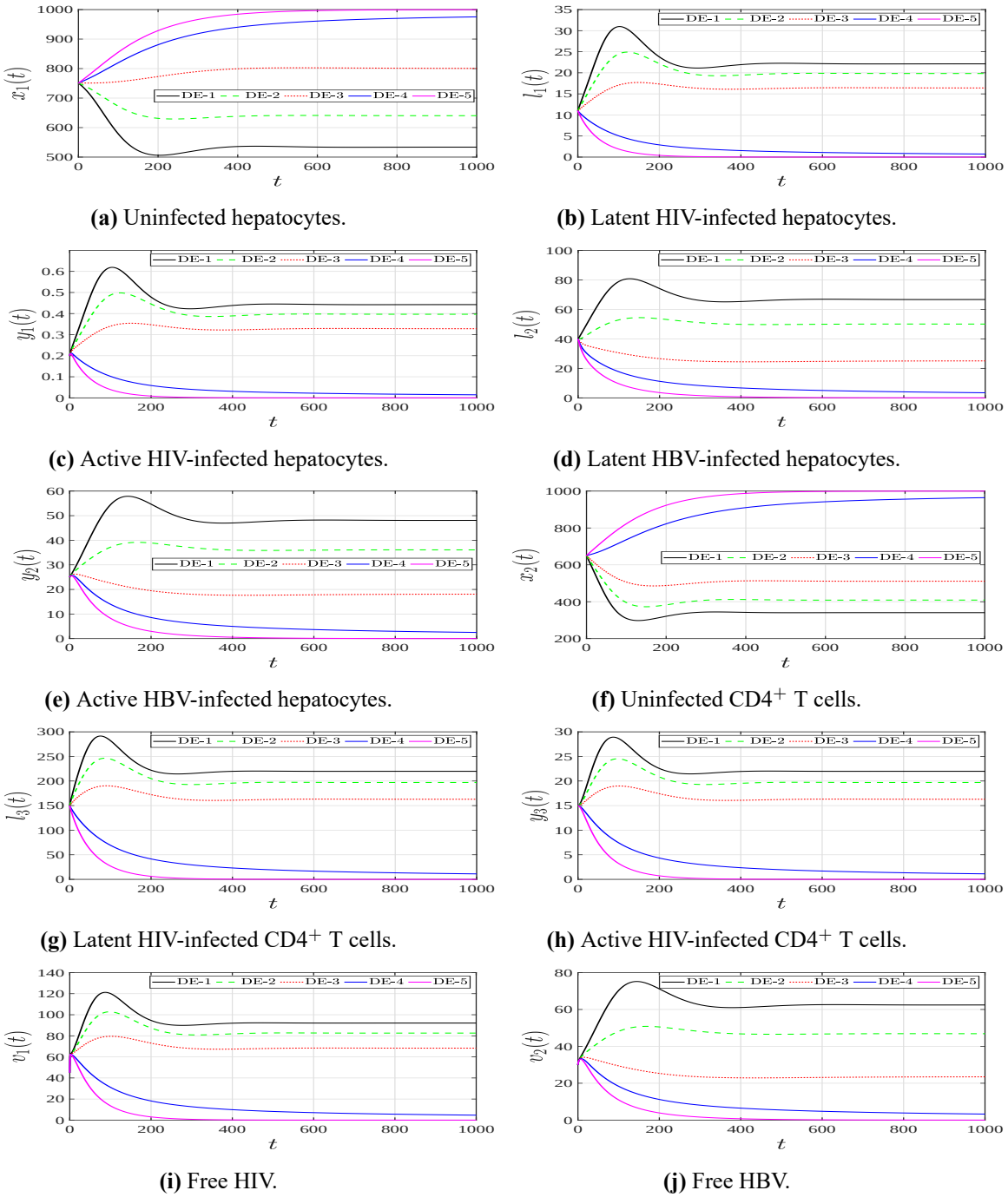

(a) Uninfected hepatocytes. **(b)** Latent HIV-infected hepatocytes.

(c) Active HIV-infected hepatocytes. **(d)** Latent HBV-infected hepatocytes.

(e) Active HBV-infected hepatocytes. **(f)** Uninfected CD4$^+$ T cells.

(g) Latent HIV-infected CD4$^+$ T cells. **(h)** Active HIV-infected CD4$^+$ T cells.

(i) Free HIV. **(j)** Free HBV.

Figure 8. Solutions of system (13)–(22) for different antiviral effectiveness rates, ϵ_1 and ϵ_2.

5.3.1. Comparison results

An analysis of the dynamics of HBV and HIV co-infection in the presence of latent reservoirs is presented. To investigate the impact of latent reservoirs on the minimum drug efficacies necessary for stabilization of infection-free equilibrium point, we consider the following model without latent reservoirs:

$$\dot{x}_1 = \lambda_1 - d_1 x_1 - (1-\epsilon_1)p\beta_1 x_1 v_1 - (1-\epsilon_2)\beta_2 x_1 v_2 \tag{23}$$

$$\dot{y}_1 = (1-\epsilon_1)p\beta_1 x_1 v_1 - a_1 y_1 \tag{24}$$

$$\dot{y}_2 = (1-\epsilon_2)\beta_2 x_1 v_2 - a_2 y_2 \tag{25}$$

$$\dot{x}_2 = \lambda_2 - d_2 x_2 - (1-\epsilon_1)(1-p)\beta_3 x_2 v_1 \tag{26}$$

$$\dot{z}_1 = (1-\epsilon_1)(1-p)\beta_3 x_2 v_1 - a_3 z_1 \tag{27}$$

$$\dot{v}_1 = k_1 a_1 y_1 + k_3 a_3 z_1 - c_1 v_1 \tag{28}$$

$$\dot{v}_2 = k_2 a_2 y_2 - c_2 v_2. \tag{29}$$

The basic reproductive numbers of system (23)–(29) are given by

$$\tilde{\mathcal{R}}_0(\epsilon_1) = \frac{k_1(1-\epsilon_1)p\beta_1\lambda_1}{c_1 d_1} + \frac{k_3(1-\epsilon_1)(1-p)\beta_3\lambda_2}{c_1 d_2} = (1-\epsilon_1)\tilde{\mathcal{R}}_0(0)$$
$$\text{and } \tilde{\mathcal{R}}_1(\epsilon_2) = \frac{k_2(1-\epsilon_2)\beta_2\lambda_1}{c_2 d_1} = (1-\epsilon_2)\tilde{\mathcal{R}}_1(0).$$

Here, $\tilde{\mathcal{R}}_0(0)$ and $\tilde{\mathcal{R}}_1(0)$ are the basic reproductive numbers of model (23)–(29) in the absence of treatment. Given that $\tilde{\mathcal{R}}_0(0) > 1$ and $\tilde{\mathcal{R}}_1(0) > 1$, and let's calculate the threshold drug efficacies $\tilde{\epsilon}_1^{\text{th}}$ and $\tilde{\epsilon}_2^{\text{th}}$ as follows:

$$\tilde{\mathcal{R}}_0(\tilde{\epsilon}_1^{\text{th}}) = 1 \Rightarrow \tilde{\epsilon}_1^{\text{th}} = 1 - \frac{1}{\tilde{\mathcal{R}}_0(0)}$$
$$\tilde{\mathcal{R}}_1(\tilde{\epsilon}_2^{\text{th}}) = 1 \Rightarrow \tilde{\epsilon}_2^{\text{th}} = 1 - \frac{1}{\tilde{\mathcal{R}}_1(0)}.$$

Then we obtain

$$\tilde{\mathcal{R}}_0(\epsilon_1) \leq 1 \text{ for all } \tilde{\epsilon}_1^{\text{th}} \leq \epsilon_1 \leq 1$$
$$\tilde{\mathcal{R}}_1(\epsilon_2) \leq 1 \text{ for all } \tilde{\epsilon}_2^{\text{th}} \leq \epsilon_2 \leq 1$$

We have

$$\mathcal{R}_0(0) = \frac{k_1 p\beta_1\lambda_1}{c_1 d_1}\frac{\eta_1}{\mu_1+\eta_1} + \frac{k_3(1-p)\beta_3\lambda_2}{c_1 d_2}\frac{\eta_3}{\mu_3+\eta_3} < \frac{k_1 p\beta_1\lambda_1}{c_1 d_1} + \frac{k_3(1-p)\beta_3\lambda_2}{c_1 d_2} = \tilde{\mathcal{R}}_0(0)$$
$$\mathcal{R}_1(0) = \frac{k_2\beta_2\lambda_1}{c_2 d_1}\frac{\eta_2}{\mu_2+\eta_2} < \frac{k_2\beta_2\lambda_1}{c_2 d_1} = \tilde{\mathcal{R}}_1(0).$$

The presence of latent reservoirs contributes to a decrease in the basic reproductive numbers in the co-infection model, effectively limiting the potential for sustained viral transmission. If these reservoirs are overlooked during the modeling process, it can result in an inflated estimation of the reproductive numbers, leading to inaccurate predictions of infection dynamics. In comparison, we find that $\epsilon_1^{\text{th}} < \tilde{\epsilon}_1^{\text{th}}$ and $\epsilon_2^{\text{th}} < \tilde{\epsilon}_2^{\text{th}}$. This suggests that incorporating latent reservoirs into the model reduces the amount of antiviral medication needed to stabilize the infection-free equilibrium point, $\mathcal{EP}_0$, and clear the co-infection. Therefore, incorporating latent reservoirs into the model is crucial for achieving a realistic and balanced understanding of the co-infection's behavior and for informing appropriate therapeutic strategies.

6. Conclusion and future directions

The presence of multiple chronic viral infections can greatly affect a patient's health. HIV and HBV are among the viruses that may simultaneously infect an individual due to their common transmission pathways. This study introduces a model for HIV-HBV co-infection within a host, where HBV predominantly infects liver cells, whereas HIV targets both $CD4^+$ T cells and hepatocytes. The model was formulated using ten nonlinear differential equations to describe the dynamics between various cell populations and viruses, including uninfected hepatocytes, latent HIV-infected hepatocytes, active HIV-infected hepatocytes, latent HBV-infected hepatocytes, active HBV-infected hepatocytes, uninfected $CD4^+$ T cells, latent HIV-infected $CD4^+$ T cells, active HIV-infected $CD4^+$ T cells, free HIV, and free HBV. Nonnegativity and boundedness of solutions were established. We determined four equilibrium states in the HIV-HBV co-infection model and established four threshold parameters. $\mathcal{R}_i$, $i = 0, 1, 2, 3$. Using the Lyapunov method and LaSalle's invariance principle, the global asymptotic stability of the four equilibria is demonstrated. We demonstrated the following:

- The infection-free equilibrium $\mathcal{E}_0$ is always present and is GAS when $\mathcal{R}_0 \leq 1$ and $\mathcal{R}_1 \leq 1$. This represents a healthy state where both HIV and HBV are expected to be eradicated.
- The HIV mono-infection equilibrium $\bar{\mathcal{E}}$ occurs when $\mathcal{R}_0 > 1$ and is GAS if $\mathcal{R}_1 \leq 1 + \frac{p\beta_1\bar{v}_1}{d_1}$ holds. This corresponds to a situation where the body is infected exclusively with HIV.
- The HBV mono-infection equilibrium $\tilde{\mathcal{E}}$ exists when $\mathcal{R}_1 > 1$ and is GAS if $\frac{\mathcal{R}_{01}}{\mathcal{R}_1} + \mathcal{R}_{02} \leq 1$ holds. In this case, the body is infected solely with HBV.
- The HIV-HBV co-infection equilibrium $\mathcal{E}^*$ occurs and is GAS when $\mathcal{R}_1 > \mathcal{R}_{01}$, $\mathcal{R}_2 > 1$, and $\mathcal{R}_3 > 1$. This scenario models the co-infection of HIV and HBV.

To validate these theoretical results, numerical simulations were carried out. A sensitivity analysis was conducted on the basic reproductive numbers for HIV ($\mathcal{R}_0$) and HBV ($\mathcal{R}_1$) infections to determine the key factors affecting the progression of HIV-HBV co-infection. Additionally, the impact of antiviral treatments targeting HIV and HBV was examined, revealing the minimum efficacy levels required for complete viral clearance. Effective antiviral treatments play a significant role in enhancing immune function and promoting liver health.

The analyzed model incorporates multiple clinical scenarios, such as a patient who has overcome a viral infection, an individual with chronic HIV infection, another with chronic HBV infection, and a patient experiencing long-term co-infection with both viruses.

This study employed a deterministic modeling framework to investigate the within-host dynamics of HIV-HBV co-infection. While this approach effectively captures average behaviors and key interactions between viruses and host cells, it does not account for the intrinsic randomness found in biological processes–such as immune response variability and stochastic cellular behavior. Incorporating a stochastic perspective would allow for a more nuanced and realistic representation by

considering random events and probabilistic mechanisms. However, due to the added mathematical and computational complexity, this extension falls outside the scope of the present work. We recognize it as a promising avenue for future exploration and plan to expand the model accordingly.

Additionally, there are several potential directions for further development of the model: (i) incorporating partial differential equations to represent spatial aspects such as cell movement and tissue structure, and (ii) integrating fractional differential equations to better reflect the effects of immunological memory. Another important future step is to validate the model's predictions by comparing them with clinical data from individuals co-infected with HIV and HBV.

Author contributions: Conceptualization, AE; methodology, AH; investigation, AA; formal analysis, AE and AA; writing original draft, AH. All authors have read and agreed to the published version of the manuscript.

Institutional review board statement: Not applicable.

Informed consent statement: Not applicable.

Conflict of interest: The authors declare no conflict of interest.

References

1. Wodarz D, Levy DN. Human immunodeficiency virus evolution towards reduced replicative fitness in vivo and the development of AIDS. Proceedings of the Royal Society B: Biological Sciences. 2007; 274(1624): 2481–2491.
2. Zerbato JM, Avihingsanon A, Singh KP, et al. HIV DNA persists in hepatocytes in people with HIV-hepatitis B co-infection on antiretroviral therapy. Bulletin of Mathematical Biology. 2023; 87: 104391.
3. Blackard JT, Sherman KE. HCV/HIV co-infection: time to re-evaluate the role of HIV in the liver. Journal of Viral Hepatitis. 2008; 15(5): 323–330.
4. UNAIDS: Global HIV&AIDS statistics-Fact sheet. Available online: https://www.unaids.org/sites/default/files/media_asset/UNAIDS_FactSheet_en.pdf (accessed on 20 February 2025).
5. Seeger C, Mason WS. Hepatitis B virus biology. Microbiology and Molecular Biology Reviews. 2000; 64(1): 51–68.
6. Gourley SA, Kuang Y, Nagy JD. Dynamics of a delay differential equation model of hepatitis B virus infection. Journal of Biological Dynamics. 2008; 2(2): 140–153.
7. World Health Organization. Hepatitis B. Available online: https://www.who.int/news-room/fact-sheets/detail/hepatitis-b (accessed on 20 February 2025).
8. Holmes KK, Sparling PF, Stamm WE, et al. Sexually transmitted diseases, 4th ed. McGraw Hill; 2008.
9. Qesmi R, Wu J, Wu J, Heffernan JM. Influence of backward bifurcation in a model of hepatitis B and C viruses. Mathematical Biosciences. 2010; 224: 118–125.
10. Corcorran MA, Kim HN. Chronic hepatitis B and HIV coinfection. Topics in Antiviral Medicine. 2023; 31(1): 14.
11. Ullah MA, Raza N, Omame A, Alqarni MS. A new co-infection model for HBV and HIV with vaccination and asymptomatic transmission using actual data from Taiwan. Physica Scripta. 2024; 99(6).
12. Wang Y, Li Y, Chen X, Zhao L. HIV-1/HBV coinfection accurate multitarget prediction using a graph neural network-based ensemble predicting model. International Journal of Molecular Sciences. 2023; 24(8): 7139.
13. Phung BC, Sogni P, Launay O. Hepatitis B and human immunodeficiency virus co-infection. World Journal of Gastroenterology: WJG. 2014; 20(46): 17360.
14. Hogan G, Winer BY, Ahodantin J, et al. Persistent hepatitis B virus and HIV coinfections in dually humanized mice engrafted with human liver and immune system. Journal of Medical Virology. 2023; 95(7): e28930.
15. Anam V, Guerrero BV, Srivastav AK, et al. Within-host models unravelling the dynamics of dengue reinfections. Infectious Disease Modelling. 2024; 9(2): 458–473.

16. Nowak MA, Bangham CRM. Population dynamics of immune responses to persistent viruses. Science. 1996; 272: 74–79.
17. Tan M, Lan G, Wei C. Dynamic analysis of HIV infection model with CTL immune response and cell-to-cell transmission. Applied Mathematics Letters. 2024; 156: 109140.
18. Lv L, Yang J, Hu Z, Fan D. Dynamics analysis of a delayed HIV model with latent reservoir and both viral and cellular infections. Mathematical Methods in the Applied Sciences. 2024.
19. Culshaw RV, Ruan S. A delay-differential equation model of HIV infection of $CD4^+$ T-cells. Mathematical Biosciences. 2000; 165: 27–39.
20. Callaway DS, Perelson AS. HIV-1 infection and low steady state viral loads. Bulletin of Mathematical Biology. 2002; 64(1): 29–64.
21. Bellomo N, Painter KJ, Tao Y, Winkler M. Occurrence vs. Absence of taxis-driven instabilities in a May-Nowak model for virus infection. SIAM Journal on Applied Mathematics. 2019; 79(5): 1990–2010.
22. Lyu G, Wang J, Zhang R. Threshold dynamics of a diffusive HIV infection model with infection-age, latency and cell–cell transmission. Communications in Nonlinear Science and Numerical Simulation. 2024; 138: 108248.
23. Nowak MA, Bonhoeffer S, Hill AM, et al. Viral dynamics in hepatitis B virus infection. Proceedings of the National Academy of Sciences. 1996; 93(9): 4398–4402.
24. Foko S. Dynamical analysis of a general delayed HBV infection model with capsids and adaptive immune response in presence of exposed infected hepatocytes. Journal of Mathematical Biology. 2024; 88(6): 75.
25. Prakash M, Rakkiyappan R, Manivannan A, et al. Stability and bifurcation analysis of hepatitis B-type virus infection model. Mathematical Methods in the Applied Sciences. 2021; 44(8): 6462–6481.
26. Din A. Bifurcation analysis of a delayed stochastic HBV epidemic model: Cell-to-cell transmission. Chaos, Solitons & Fractals. 2024; 181: 114714.
27. Yaagoub Z, Sadki M, Allali K. A generalized fractional hepatitis B virus infection modelwith both cell-to-cell and virus-to-cell transmissions. Nonlinear Dynamics. 2024; 112: 16559–16585.
28. Wang K, Wang W. Propagation of HBV with spatial dependence. Mathematical Biosciences. 2007; 210: 78–95.
29. Liu L, Ma X, Li Y, Liu X. Mathematical analysis of global dynamics and optimal control of treatment for an age-structured HBV infection model. Chaos, Solitons & Fractals. 2023; 177: 114240.
30. Li W, Liu X, Lang Y. Numerical analysis of a nonlinear age-structured HBV model with saturated incidence and spatial diffusion. Mathematics and Computers in Simulation. 2024; 225: 250–266.
31. Yosyingyong P, Viriyapong R. Global dynamics of multiple delays within-host model for a hepatitis B virus infection of hepatocytes with immune response and drug therapy. Mathematical Biosciences and Engineering. 2023; 20(4): 7349–7386.
32. Ciupe SM, Ribeiro RM, Nelson PW, Perelson AS. Modeling the mechanisms of acute hepatitis B virus infection. Journal of Theoretical Biology. 2007; 247(1): 23–35.
33. Song B, Zhang Y, Sang Y, Zhang L. Stability and Hopf bifurcation on an immunity delayed HBV/HCV model with intra-and extra-hepatic coinfection and saturation incidence. Nonlinear Dynamics. 2023; 111(15): 14485–14511.
34. Yaagoub Z, Allali K. Fractional HBV infection model with both cell-to-cell and virus-to-cell transmissions and adaptive immunity. Chaos, Solitons & Fractals. 2022; 165(Part 1): 112855.
35. Li M, Zu J. The review of differential equation models of HBV infection dynamics. Journal of Virological Methods. 2019; 266: 103–113.
36. Bowong S, Kamganga J, Tewa J, Tsanou B. Modelling and analysis of hepatitis B and HIV co-infections. In: Proceedings of the 10th African Conference on Research in Computer Science and Applied Mathematics; Day month 2010; City, Country. pp. 109–116.
37. Endashaw EE, Mekonnen TT. Modeling the effect of vaccination and treatment on the transmission dynamics of hepatitis b virus and hiv/aids coinfection. Journal of Applied Mathematics. 2022.
38. Endashaw EE, Gebru DM, Alemneh HT. Coinfection dynamics of HBV-HIV/AIDS with mother-to-child transmission and medical interventions. Computational and Mathematical Methods in Medicine. 2022; (1): 4563577.
39. Nampala H, Luboobi LS, Mugisha JY, et al. Modelling hepatotoxicity and antiretroviral therapeutic effect in HIV/HBV co-infection. Mathematical Biosciences. 2018; 302: 67–79.
40. Nampala H, Jablonska-Sabuka M, Singull M. Mathematical analysis of the role of HIV/HBV latency in hepatocytes. Journal of Applied Mathematics. 2021; 2021(1): 5525857.
41. Guo T, Qiu Z, Shen M, Rong L. Dynamics of a new HIV model with the activation status of infected cells. Journal of Mathematical Biology. 2021; 82(6): 51.

42. Perelson AS, Essunger P, Cao Y, Vesanen M, et al. Decay characteristics of HIV-1-infected compartments during combination therapy. Nature. 1997; 387(6629): 188–191.
43. Guo T, Deng Q, Gao S, et al. HIV infection dynamics with broadly neutralizing antibodies and CTL immune response. Discrete and Continuous Dynamical Systems-S. 2024. doi: 10.3934/dcdss.2024151
44. Zhang Z, Chen Y, Wang X, Rong L. Dynamic analysis of a latent HIV infection model with CTL immune and antibody responses. International Journal of Biomathematics. 2024; 17(03): 2350079.
45. Van den Driessche P, Watmough J. Reproduction numbers and sub-threshold endemic equilibria for compartmental models of disease transmission. Mathematical Biosciences. 2002; 180(1–2): 29–48.
46. Korobeinikov A. Global properties of basic virus dynamics models. Bulletin of Mathematical Biology. 2004; 66(4): 879–883.
47. Wodarz D. Mathematical models of immune effector responses to viral infections: Virus control versus the development of pathology. Journal of Computational and Applied Mathematics. 2005; 184(1): 301–319.
48. Webster G, Reignat S, Maini M, et al. Incubation phase of acute hepatitis B in man: Dynamic of cellular immune mechanisms. Hepatology. 2000; 32(5): 1117–1124.
49. Mohri H, Bonhoeffer S, Monard S, et al. Rapid turnover of T lymphocytes in SIV-infected rhesus macaques. Science. 1998; 279: 1223–1227.
50. Dahari H, Lo A, Ribeiro R, Perelson A. Modeling hepatitis C virus dynamics: Liver regeneration and critical drug efficacy. Journal of Theoretical Biology. 2007; 247(2): 371–381.
51. Yousfi N, Hattaf K, Tridane A. Modeling the adaptive immune response in HBV infection. Journal of Mathematical Biology. 2011; 63: 933–957.
52. Haase AT, Henry K, Zupancic M, et al. Quantitative image analysis of HIV-1 infection in lymphoid tissue. Science. 1996; 274(5289): 985–989.
53. Perelson AS, Kirschner DE, De Boer R. Dynamics of HIV infection of CD4+ T cells. Mathematical Biosciences. 1993; 114(1): 81–125.
54. Wang Y, Zhou Y, Wu J, Heffernan J. Oscillatory viral dynamics in a delayed HIV pathogenesis model. Mathematical Biosciences. 2009; 219(2): 104–112.
55. Tsiang M, Rooney J, Toole J, Gibbs C. Biphasic clearance kinetics of hepatitis B virus from patients during adefovir dipivoxil therapy. Hepatology. 1999; 29: 1863–1869.
56. Harroudi S, Meskaf A, Allali K. Modelling the adaptive immune response in HBV infection model with HBV DNA-containing capsids. Differential Equations and Dynamical Systems. 2023; 31: 371–393.
57. Sahani SK, Yashi A. A delayed HIV infection model with apoptosis and viral loss. Journal of biological dynamics. 2018; 12(1): 1012–1034.
58. Pankavich S. The effects of latent infection on the dynamics of HIV-1. Differential Equations and Dynamical Systems. 2016; 24(3): 281–303.
59. Marino S, Hogue IB, Ray CJ, Kirschner DE. A methodology for performing global uncertainty and sensitivity analysis in systems biology. Journal of Theoretical Biology. 2008; 254: 178–196.
60. Lewin SR, Ribeiro RM, Walters T, et al. Analysis of hepatitis B viral load decline under potent therapy: complex decay profiles observed. Hepatology. 2001; 34(5): 1012–1020.
61. Hale JK, Verduyn Lunel SM. Introduction to Functional Differential Equations. Springer-Verlag; 1993.
62. Khalil HK. Nonlinear Systems, 3rd ed. Prentice Hall; 2002.

Appendix A

I. Basic reproductive number

The basic reproductive number represents the average number of secondary infections generated by a single infected cell during its infectious period, assuming all target cells are initially uninfected [39]. This threshold is determined at the infection-free equilibrium.

i. Computation of the basic reproductive number for HIV mono-infection

HIV mono-infection model is obtained by setting $v_2 = l_2 = y_2 = 0$ in Equations (1)–(10) as:

$$\dot{x}_1 = \lambda_1 - d_1 x_1 - p\beta_1 x_1 v_1 \tag{A1}$$
$$\dot{l}_1 = p\beta_1 x_1 v_1 - (\mu_1 + \eta_1) l_1 \tag{A2}$$
$$\dot{y}_1 = \eta_1 l_1 - a_1 y_1 \tag{A3}$$
$$\dot{x}_2 = \lambda_2 - d_2 x_2 - (1-p)\beta_3 x_2 v_1 \tag{A4}$$
$$\dot{l}_3 = (1-p)\beta_3 x_2 v_1 - (\mu_3 + \eta_3) l_3 \tag{A5}$$
$$\dot{y}_3 = \eta_3 l_3 - a_3 y_3 \tag{A6}$$
$$\dot{v}_1 = k_1 a_1 y_1 + k_3 a_3 y_3 - c_1 v_1, \tag{A7}$$

The infection-free equilibrium of system (A1)–(A7) is given by $\mathcal{E}_0 = \left(x_1^0, 0, 0, x_2^0, 0, 0, 0\right)$. The basic reproductive number, $\mathcal{R}_0$, is computed as the spectral radius (i.e., the largest eigenvalue) of the next-generation matrix, given by $\rho(F_0 V_0^{-1})$, where F_0 is the infection matrix and V_0 is the transition matrix derived from the system of equations [45]. Matrices F_0 and V_0 are given by

$$F_0 = \begin{pmatrix} 0 & 0 & 0 & 0 & \frac{p\beta_1\lambda_1}{d_1} \\ 0 & 0 & 0 & 0 & 0 \\ 0 & 0 & 0 & 0 & \dfrac{(1-p)\beta_3\lambda_2}{d_2} \\ 0 & 0 & 0 & 0 & 0 \\ 0 & 0 & 0 & 0 & 0 \end{pmatrix}, \; V_0 = \begin{pmatrix} \mu_1+\eta_1 & 0 & 0 & 0 & 0 \\ -\eta_1 & a_1 & 0 & 0 & 0 \\ 0 & 0 & \mu_3+\eta_3 & 0 & 0 \\ 0 & 0 & -\eta_3 & a_3 & 0 \\ 0 & -a_1 k_1 & 0 & -a_3 k_3 & c_1 \end{pmatrix}.$$

Therefore

$$\mathcal{R}_0 = \rho(F_0 V_0^{-1}) = \mathcal{R}_{01} + \mathcal{R}_{02}$$

where

$$\mathcal{R}_{01} = \frac{k_1 p\beta_1\lambda_1}{c_1 d_1}\frac{\eta_1}{\mu_1+\eta_1}$$
$$\mathcal{R}_{02} = \frac{k_3(1-p)\beta_3\lambda_2}{c_1 d_2}\frac{\eta_3}{\mu_3+\eta_3}.$$

Given that HIV targets both hepatocytes and CD4$^+$ T cells, $\mathcal{R}_{01}$ represents the average number of new infections generated by HIV within hepatocytes, whereas $\mathcal{R}_{02}$ corresponds to the number of secondary infections occurring in CD4$^+$ T cells.

ii. Computation of the basic reproductive number for HBV mono-infection

HIV mono-infection model is obtained by setting $v_1 = l_1 = l_3 = y_1 = y_3 = 0$ in Equations (1)–(10) as:

$$\dot{x}_1 = \lambda_1 - d_1 x_1 - \beta_2 x_1 v_2, \tag{A8}$$

$$\dot{l}_2 = \beta_2 x_1 v_2 - (\mu_2 + \eta_2) l_2, \tag{A9}$$

$$\dot{y}_2 = \eta_2 l_2 - a_2 y_2, \tag{A10}$$

$$\dot{v}_2 = k_2 a_2 y_2 - c_2 v_2. \tag{A11}$$

Following a method analogous to that used for the HIV-only case, we determine $\mathcal{R}_1$, the basic reproductive number for HBV mono-infection, through the next-generation matrix framework [45]. To proceed, we define the following matrices:

$$F_1 = \begin{pmatrix} 0 & 0 & \frac{\beta_2 \lambda_1}{d_1} \\ 0 & 0 & 0 \\ 0 & 0 & 0 \end{pmatrix}, \; V_1 = \begin{pmatrix} \mu_2 + \eta_2 & 0 & 0 \\ -\eta_2 & a_2 & 0 \\ 0 & -a_2 k_2 & c_2 \end{pmatrix}.$$

Hence

$$\mathcal{R}_1 = \rho(F_1 V_1^{-1}) = \frac{k_2 \beta_2 \lambda_1}{c_2 d_1} \frac{\eta_2}{\mu_2 + \eta_2}.$$

Here, $\mathcal{R}_1$ represents the average number of new infections generated by HBV within hepatocytes.

iii. Computation of the basic reproductive number for HBV-HIV co-infection

We consider the co-infection model (1)–(10), and we calculate the basic reproductive number $\mathcal{R}_{Co}$ as $\mathcal{R}_{Co} = \rho(F_{Co} V_{Co}^{-1})$, where

$$F_{Co} = \begin{pmatrix} 0 & 0 & 0 & 0 & 0 & 0 & \frac{p\beta_1\lambda_1}{d_1} & 0 \\ 0 & 0 & 0 & 0 & 0 & 0 & 0 & 0 \\ 0 & 0 & 0 & 0 & 0 & 0 & 0 & \frac{\beta_2\lambda_1}{d_1} \\ 0 & 0 & 0 & 0 & 0 & 0 & 0 & 0 \\ 0 & 0 & 0 & 0 & 0 & 0 & \frac{(1-p)\beta_3\lambda_2}{d_2} & 0 \\ 0 & 0 & 0 & 0 & 0 & 0 & 0 & 0 \\ 0 & 0 & 0 & 0 & 0 & 0 & 0 & 0 \\ 0 & 0 & 0 & 0 & 0 & 0 & 0 & 0 \end{pmatrix}$$

$$V_{Co} = \begin{pmatrix} \mu_1 + \eta_1 & 0 & 0 & 0 & 0 & 0 & 0 & 0 \\ -\eta_1 & a_1 & 0 & 0 & 0 & 0 & 0 & 0 \\ 0 & 0 & \mu_2 + \eta_2 & 0 & 0 & 0 & 0 & 0 \\ 0 & 0 & -\eta_2 & a_2 & 0 & 0 & 0 & 0 \\ 0 & 0 & 0 & 0 & \mu_3 + \eta_3 & 0 & 0 & 0 \\ 0 & 0 & 0 & 0 & -\eta_3 & a_3 & 0 & 0 \\ 0 & -a_1 k_1 & 0 & 0 & 0 & -a_3 k_3 & c_1 & 0 \\ 0 & 0 & 0 & -a_2 k_2 & 0 & 0 & 0 & c_2 \end{pmatrix}$$

Therefore,

$$\begin{aligned} \mathcal{R}_{Co} = \rho(F_{Co} V_{Co}^{-1}) &= \max\left\{ \frac{k_1 p \beta_1 \lambda_1}{c_1 d_1} \frac{\eta_1}{\mu_1 + \eta_1} + \frac{k_3 (1-p) \beta_3 \lambda_2}{c_1 d_2} \frac{\eta_3}{\mu_3 + \eta_3}, \frac{k_2 \beta_2 \lambda_1}{c_2 d_1} \frac{\eta_2}{\mu_2 + \eta_2} \right\} \\ &= \max\{\mathcal{R}_0, \mathcal{R}_1\}. \end{aligned}$$

Appendix B

Proofs of global stability

Proof. Consider $\mathcal{F}_0(x_1, l_1, y_1, l_2, y_2, x_2, l_3, y_3, v_1, v_2)$

$$\begin{aligned}\mathcal{F}_0 = x_1 - x_1^0 - x_1^0 \ln\left(\frac{x_1}{x_1^0}\right) + l_1 + \frac{\mu_1+\eta_1}{\eta_1}y_1 + l_2 + \frac{\mu_2+\eta_2}{\eta_2}y_2 \\ + \frac{k_3\eta_3(\mu_1+\eta_1)}{k_1\eta_1(\mu_3+\eta_3)}\left(x_2 - x_2^0 - x_2^0\ln\left(\frac{x_2}{x_2^0}\right)\right) + \frac{k_3\eta_3(\mu_1+\eta_1)}{k_1\eta_1(\mu_3+\eta_3)}l_3 \\ + \frac{k_3(\mu_1+\eta_1)}{k_1\eta_1}y_3 + \frac{(\mu_1+\eta_1)}{k_1\eta_1}v_1 + \frac{(\mu_2+\eta_2)}{k_2\eta_2}v_2.\end{aligned}$$

Calculating $\dfrac{d\mathcal{F}_0}{dt}$ along the solution of system (1)–(10) as

$$\begin{aligned}\frac{d\mathcal{F}_0}{dt} = \left(1-\frac{x_1^0}{x_1}\right)\dot{x}_1 + \dot{l}_1 + \frac{\mu_1+\eta_1}{\eta_1}\dot{y}_1 + \dot{l}_2 + \frac{\mu_2+\eta_2}{\eta_2}\dot{y}_2 + \frac{k_3\eta_3(\mu_1+\eta_1)}{k_1\eta_1(\mu_3+\eta_3)}\left(1-\frac{x_2^0}{x_2}\right)\dot{x}_2 \\ + \frac{k_3\eta_3(\mu_1+\eta_1)}{k_1\eta_1(\mu_3+\eta_3)}\dot{l}_3 + \frac{k_3(\mu_1+\eta_1)}{k_1\eta_1}\dot{y}_3 + \frac{(\mu_1+\eta_1)}{k_1\eta_1}\dot{v}_1 + \frac{(\mu_2+\eta_2)}{k_2\eta_2}\dot{v}_2.\end{aligned}$$

From Equations (1)–(10) we obtain

$$\begin{aligned}\frac{d\mathcal{F}_0}{dt} &= \left(1-\frac{x_1^0}{x_1}\right)(\lambda_1 - d_1x_1 - p\beta_1x_1v_1 - \beta_2x_1v_2) + p\beta_1x_1v_1 - (\mu_1+\eta_1)l_1 + \frac{\mu_1+\eta_1}{\eta_1}(\eta_1l_1 - a_1y_1) \\ &+ \beta_2x_1v_2 - (\mu_2+\eta_2)l_2 + \frac{\mu_2+\eta_2}{\eta_2}(\eta_2l_2 - a_2y_2) \\ &+ \frac{k_3\eta_3(\mu_1+\eta_1)}{k_1\eta_1(\mu_3+\eta_3)}\left(1-\frac{x_2^0}{x_2}\right)(\lambda_2 - d_2x_2 - (1-p)\beta_3x_2v_1) \\ &+ \frac{k_3\eta_3(\mu_1+\eta_1)}{k_1\eta_1(\mu_3+\eta_3)}((1-p)\beta_3x_2v_1 - (\mu_3+\eta_3)l_3) + \frac{k_3(\mu_1+\eta_1)}{k_1\eta_1}(\eta_3l_3 - a_3y_3) \\ &+ \frac{(\mu_1+\eta_1)}{k_1\eta_1}(k_1a_1y_1 + k_3a_3y_3 - c_1v_1) + \frac{(\mu_2+\eta_2)}{k_2\eta_2}(k_2a_2y_2 - c_2v_2) \\ &= \left(1-\frac{x_1^0}{x_1}\right)(\lambda_1 - d_1x_1) + p\beta_1x_1^0v_1 + \beta_2x_1^0v_2 \\ &+ \frac{k_3\eta_3(\mu_1+\eta_1)}{k_1\eta_1(\mu_3+\eta_3)}\left(1-\frac{x_2^0}{x_2}\right)(\lambda_2 - d_2x_2) \\ &+ \frac{k_3\eta_3(\mu_1+\eta_1)}{k_1\eta_1(\mu_3+\eta_3)}(1-p)\beta_3x_2^0v_1 \\ &- \frac{(\mu_1+\eta_1)}{k_1\eta_1}c_1v_1 - \frac{(\mu_2+\eta_2)}{k_2\eta_2}c_2v_2 \\ &= -\frac{d_1}{x_1}\left(x_1-x_1^0\right)^2 - \frac{d_2k_3\eta_3(\mu_1+\eta_1)}{x_2k_1\eta_1(\mu_3+\eta_3)}\left(x_2-x_2^0\right)^2 \\ &+ p\beta_1x_1^0v_1 + \beta_2x_1^0v_2 + \frac{k_3\eta_3(\mu_1+\eta_1)}{k_1\eta_1(\mu_3+\eta_3)}(1-p)\beta_3x_2^0v_1 - \frac{(\mu_1+\eta_1)}{k_1\eta_1}c_1v_1 - \frac{(\mu_2+\eta_2)}{k_2\eta_2}c_2v_2.\end{aligned}$$

Collecting terms as

$$\begin{aligned}\frac{d\mathcal{F}_0}{dt} = &-\frac{d_1}{x_1}\left(x_1 - x_1^0\right)^2 - \frac{d_2k_3\eta_3(\mu_1+\eta_1)}{x_2k_1\eta_1(\mu_3+\eta_3)}\left(x_2 - x_2^0\right)^2 \\ &+ \frac{c_1(\mu_1+\eta_1)}{k_1\eta_1}\left(\frac{k_1\eta_1 p\beta_1 x_1^0}{c_1(\mu_1+\eta_1)} + \frac{k_3\eta_3(1-p)\beta_3 x_2^0}{c_1(\mu_3+\eta_3)} - 1\right)v_1 \\ &+ \frac{c_2(\mu_2+\eta_2)}{k_2\eta_2}\left(\frac{k_2\eta_2\beta_2 x_1^0}{c_2(\mu_2+\eta_2)} - 1\right)v_2.\end{aligned}$$

Finally, we obtain

$$\begin{aligned}\frac{d\mathcal{F}_0}{dt} = &-\frac{d_1}{x_1}\left(x_1 - x_1^0\right)^2 - \frac{d_2k_3\eta_3(\mu_1+\eta_1)}{x_2k_1\eta_1(\mu_3+\eta_3)}\left(x_2 - x_2^0\right)^2 + \frac{c_1(\mu_1+\eta_1)}{k_1\eta_1}\left(\mathcal{R}_0 - 1\right)v_1 \\ &+ \frac{c_2(\mu_2+\eta_2)}{k_2\eta_2}\left(\mathcal{R}_1 - 1\right)v_2.\end{aligned}$$

Therefore, for all $x_1, l_1, y_1, l_2, y_2, x_2, l_3, y_3, v_1, v_2 > 0$ we have $\frac{d\mathcal{F}_0}{dt} \leq 0$ when $\max(\mathcal{R}_0, \mathcal{R}_1) \leq 1$. Moreover, $\frac{d\mathcal{F}_0}{dt} = 0$ when $x_1 = x_1^0$, $x_2 = x_2^0$, $(\mathcal{R}_0 - 1)v_1 = 0$, and $(\mathcal{R}_1 - 1)v_2 = 0$. According to [61], solutions of system (1)–(10) limit to Ω_0', which contains elements with $x_1(t) = x_1^0$, $x_2(t) = x_2^0$ and

$$(\mathcal{R}_0 - 1)v_1 = 0 \tag{B1}$$

$$(\mathcal{R}_1 - 1)v_2 = 0. \tag{B2}$$

Let us consider four cases:

- If $\max(\mathcal{R}_0, \mathcal{R}_1) < 1$ then from Equations (B1) and (B2), we obtain $v_1 = v_2 = 0$. Since Ω_0' is invariant we obtain $\dot{v}_1(t) = \dot{v}_2(t) = 0$. From Equations (9) and (10), we have

$$0 = \dot{v}_1 = k_1a_1y_1 + k_3a_3y_3 \Rightarrow y_1(t) = y_3(t) = 0, \text{ for any } t \tag{B3}$$

and

$$0 = \dot{v}_2 = k_2a_2y_2 = 0 \Rightarrow y_2(t) = 0, \text{ for any } t. \tag{B4}$$

Furthermore, since $y_1 = 0$ then $\dot{y}_1(t) = 0$ and thus $l_1(t) = 0$, for any t. Similarly, $y_2 = 0$ then $\dot{y}_2(t) = 0$ and thus $l_2(t) = 0$, for any t. By the same way, $y_3 = 0$ then $\dot{y}_3(t) = 0$ and thus $l_3(t) = 0$, for any t. Hence, $\Omega_0' = \{\mathcal{E}_0\}$.

- If $\mathcal{R}_0 = \mathcal{R}_1 = 1$, we have $x_1 = x_1^0$, $x_2 = x_2^0$ then $\dot{x}_1(t) = \dot{x}_2(t) = 0$. From Equations (1) and (6), we have

$$\lambda_2 - d_2x_2^0 - (1-p)\beta_3x_2^0v_1 = 0 \Rightarrow v_1(t) = 0, \text{ for any } t \tag{B5}$$

$$\lambda_1 - d_1x_1^0 - p\beta_1x_1^0v_1 - \beta_2x_1^0v_2 = 0 \Rightarrow v_2(t) = 0, \text{ for any } t \tag{B6}$$

Equations (B3) and (B4) imply $y_1(t) = y_2(t) = y_3(t) = l_1(t) = l_2(t) = l_3(t) = 0$ for all $t \geq 0$. Hence, $\Omega_0' = \{\mathcal{E}_0\}$.

- If $\mathcal{R}_0 < 1$ and $\mathcal{R}_1 = 1$, then $v_1 = 0$ and $x_1 = x_1^0$, $x_2 = x_2^0$ thus Equation (B6) gives $v_2(t) = 0$, for any t and from Equations (B3) and (B4), we get $y_1(t) = y_2(t) = y_3(t) = l_1(t) = l_2(t) = l_3(t) = 0$ for all $t \geq 0$. Hence, $\Omega_0' = \{\mathcal{E}_0\}$.
- Similarly, if $\mathcal{R}_0 = 1$ and $\mathcal{R}_1 < 1$, then $v_2 = 0$ and $x_1 = x_1^0$, $x_2 = x_2^0$ and thus Equation (B5) provides $v_1(t) = 0$, for any t. From Equations (B3) and (B4), we get $y_1(t) = y_2(t) = y_3(t) = l_1(t) = l_2(t) = l_3(t) = 0$ for all $t \geq 0$. Hence, $\Omega_0' = \{\mathcal{E}_0\}$.

LaSalle's invariance principle (LIP) [62] reveals that $\mathcal{E}_0 = \left(x_1^0, 0, 0, x_2^0, 0, 0, 0\right)$ is GAS only if $\max(\mathcal{R}_0, \mathcal{R}_1) \leq 1$.

To prove that $\mathcal{E}_0$ is unstable when $R_0 > 1$ and/or $R_1 > 1$, the Jacobian matrix $J = J(x_1, l_1, y_1, l_2, y_2, x_2, l_3, y_3, v_1, v_2)$ of model (1)–(10) is calculated as:

$$J = \begin{pmatrix} -(d_1 + p\beta_1 v_1 + \beta_2 v_2) & 0 & 0 & 0 & 0 & 0 & 0 & 0 & -p\beta_1 x_1 & -\beta_2 x_1 \\ p\beta_1 v_1 & -(\mu_1 + \eta_1) & 0 & 0 & 0 & 0 & 0 & 0 & p\beta_1 x_1 & 0 \\ 0 & \eta_1 & -a_1 & 0 & 0 & 0 & 0 & 0 & 0 & 0 \\ \beta_2 v_2 & 0 & 0 & -(\mu_2 + \eta_2) & 0 & 0 & 0 & 0 & 0 & \beta_2 x_1 \\ 0 & 0 & 0 & \eta_2 & -a_2 & 0 & 0 & 0 & 0 & 0 \\ 0 & 0 & 0 & 0 & 0 & -(d_2 + (1-p)\beta_3 v_1) & 0 & 0 & -(1-p)\beta_3 x_2 & 0 \\ 0 & 0 & 0 & 0 & 0 & (1-p)\beta_3 v_1 & -(\mu_3 + \eta_3) & 0 & (1-p)\beta_3 x_2 & 0 \\ 0 & 0 & 0 & 0 & 0 & 0 & \eta_3 & -a_3 & 0 & 0 \\ 0 & 0 & k_1 a_1 & 0 & 0 & 0 & 0 & k_3 a_3 & -c_1 & 0 \\ 0 & 0 & 0 & 0 & k_2 a_2 & 0 & 0 & 0 & 0 & -c_2 \end{pmatrix}.$$

Consequently, at $\mathcal{E}_0$,

$$J = \begin{pmatrix} -d_1 & 0 & 0 & 0 & 0 & 0 & 0 & 0 & -p\beta_1 x_1^0 & -\beta_2 x_1^0 \\ 0 & -(\mu_1 + \eta_1) & 0 & 0 & 0 & 0 & 0 & 0 & p\beta_1 x_1^0 & 0 \\ 0 & \eta_1 & -a_1 & 0 & 0 & 0 & 0 & 0 & 0 & 0 \\ 0 & 0 & 0 & -(\mu_2 + \eta_2) & 0 & 0 & 0 & 0 & 0 & \beta_2 x_1^0 \\ 0 & 0 & 0 & \eta_2 & -a_2 & 0 & 0 & 0 & 0 & 0 \\ 0 & 0 & 0 & 0 & 0 & -d_2 & 0 & 0 & -(1-p)\beta_3 x_2^0 & 0 \\ 0 & 0 & 0 & 0 & 0 & 0 & -(\mu_3 + \eta_3) & 0 & (1-p)\beta_3 x_2^0 & 0 \\ 0 & 0 & 0 & 0 & 0 & 0 & \eta_3 & -a_3 & 0 & 0 \\ 0 & 0 & k_1 a_1 & 0 & 0 & 0 & 0 & k_3 a_3 & -c_1 & 0 \\ 0 & 0 & 0 & 0 & k_2 a_2 & 0 & 0 & 0 & 0 & -c_2 \end{pmatrix}$$

and the characteristic equation is given by

$$\det(J - sI) = (s + d_1)(s + d_2)\mathcal{G}(s)\mathcal{H}(s) = 0 \tag{B7}$$

where s is the eigenvalue and

$$\mathcal{G}(s) = s^3 + A_2 s^2 + A_1 s + A_0$$
$$\mathcal{H}(s) = s^5 + B_4 s^4 + B_3 s^3 + B_2 s^2 + B_1 s + B_0$$

where

$$
\begin{aligned}
A_2 &= a_2 + c_2 + \eta_2 + \mu_2 \\
A_1 &= a_2c_2 + a_2\eta_2 + c_2\eta_2 + a_2\mu_2 + c_2\mu_2 \\
A_0 &= a_2c_2(\eta_2 + \mu_2) - \frac{a_2k_2\beta_2\eta_2\lambda_1}{d_1} \\
B_4 &= a_1 + a_3 + c_1 + \eta_1 + \eta_3 + \mu_1 + \mu_3 \\
B_3 &= c_1(\eta_1 + \eta_3 + \mu_1) + \eta_3(\eta_1 + \mu_1) + \mu_3(c_1 + \eta_1 + \mu_1) \\
&\quad + a_3(c_1 + \eta_1 + \eta_3 + \mu_1 + \mu_3) + a_1(a_3 + c_1 + \eta_1 + \eta_3 + \mu_1 + \mu_3) \\
B_2 &= c_1(\eta_1 + \mu_1)(\eta_3 + \mu_3) + a_3((\eta_1 + \mu_1)(\eta_3 + \mu_3) + c_1(\eta_1 + \eta_3 + \mu_1 + \mu_3)) \\
&\quad + a_1((\eta_1 + \mu_1)(\eta_3 + \mu_3) + c_1(\eta_1 + \eta_3 + \mu_1 + \mu_3) + a_3(c_1 + \eta_1 + \eta_3 + \mu_1 + \mu_3)) \\
&\quad - \frac{a_1k_1p\beta_1\eta_1\lambda_1}{d_1} - \frac{a_3k_3(1-p)\beta_3\eta_3\lambda_2}{d_2} \\
B_1 &= a_3c_1(\eta_1 + \mu_1)(\eta_3 + \mu_3) + a_1(c_1(\eta_1 + \mu_1)(\eta_3 + \mu_3) + a_3((\eta_1 + \mu_1)(\eta_3 + \mu_3) + c_1(\eta_1 + \eta_3 + \mu_1 + \mu_3))) \\
&\quad - \frac{a_1k_1p\beta_1\eta_1\lambda_1(a_3 + \eta_3 + \mu_3)}{d_1} - \frac{a_3k_3(1-p)\beta_3\eta_3\lambda_2(a_1 + \eta_1 + \mu_1)}{d_2} \\
B_0 &= a_1a_3c_1(\eta_1 + \mu_1)(\eta_3 + \mu_3) - \frac{a_1a_3k_1p\beta_1\eta_1\lambda_1(\eta_3 + \mu_3)}{d_1} - \frac{a_1a_3k_3(1-p)\beta_3\eta_3\lambda_2(\eta_1 + \mu_1)}{d_2}.
\end{aligned}
$$

Clearly

$$
\begin{aligned}
\mathcal{G}(0) &= a_2c_2(\eta_2 + \mu_2) - \frac{a_2k_2\beta_2\eta_2\lambda_1}{d_1} = a_2c_2(\eta_2 + \mu_2)(1 - \mathcal{R}_1) < 0 \text{ if } \mathcal{R}_1 > 1 \\
\lim_{s\to\infty} \mathcal{G}(s) &= \infty,
\end{aligned}
$$

then a positive root of $\mathcal{G}(s) = 0$ on the interval $(0, \infty)$ exists when $\mathcal{R}_1 > 1$. Similarly,

$$
\begin{aligned}
\mathcal{H}(0) &= a_1a_3c_1(\eta_1 + \mu_1)(\eta_3 + \mu_3) - \frac{a_1a_3k_1p\beta_1\eta_1\lambda_1(\eta_3 + \mu_3)}{d_1} - \frac{a_1a_3k_3(1-p)\beta_3\eta_3\lambda_2(\eta_1 + \mu_1)}{d_2} \\
&= a_1a_3c_1(\eta_1 + \mu_1)(\eta_3 + \mu_3)(1 - \mathcal{R}_0) < 0 \text{ if } \mathcal{R}_0 > 1, \\
\lim_{s\to\infty} \mathcal{H}(s) &= \infty.
\end{aligned}
$$

A positive root of $\mathcal{H}(s) = 0$ in the interval $(0, \infty)$ exists when $\mathcal{R}_0 > 1$. Therefore $\mathcal{E}_0$ is unstable when $\mathcal{R}_0 > 1$ and/or $\mathcal{R}_1 > 1$. □

Proof. Define a function $\bar{\mathcal{F}}(x_1, l_1, y_1, l_2, y_2, x_2, l_3, y_3, v_1, v_2)$

$$
\begin{aligned}
\bar{\mathcal{F}} &= x_1 - \bar{x}_1 - \bar{x}_1 \ln\left(\frac{x_1}{\bar{x}_1}\right) + l_1 - \bar{l}_1 - \bar{l}_1 \ln\left(\frac{l_1}{\bar{l}_1}\right) + \frac{\mu_1 + \eta_1}{\eta_1}\left(y_1 - \bar{y}_1 - \bar{y}_1 \ln\left(\frac{y_1}{\bar{y}_1}\right)\right) \\
&\quad + l_2 + \frac{\mu_2 + \eta_2}{\eta_2}y_2 + \frac{k_3\eta_3(\mu_1 + \eta_1)}{k_1\eta_1(\mu_3 + \eta_3)}\left(x_2 - \bar{x}_2 - \bar{x}_2 \ln\left(\frac{x_2}{\bar{x}_2}\right)\right) + \frac{k_3\eta_3(\mu_1 + \eta_1)}{k_1\eta_1(\mu_3 + \eta_3)}\left(l_3 - \bar{l}_3 - \bar{l}_3 \ln\left(\frac{l_3}{\bar{l}_3}\right)\right) \\
&\quad + \frac{k_3(\mu_1 + \eta_1)}{k_1\eta_1}\left(y_3 - \bar{y}_3 - \bar{y}_3 \ln\left(\frac{y_3}{\bar{y}_3}\right)\right) + \frac{(\mu_1 + \eta_1)}{k_1\eta_1}\left(v_1 - \bar{v}_1 - \bar{v}_1 \ln\left(\frac{v_1}{\bar{v}_1}\right)\right) + \frac{(\mu_2 + \eta_2)}{k_2\eta_2}v_2.
\end{aligned}
$$

We calculate $\frac{d\bar{\mathcal{F}}}{dt}$ as:

$$\begin{aligned}\frac{d\bar{\mathcal{F}}}{dt} &= \left(1-\frac{\bar{x}_1}{x_1}\right)(\lambda_1 - d_1x_1 - p\beta_1x_1v_1 - \beta_2x_1v_2) + \left(1-\frac{\bar{l}_1}{l_1}\right)(p\beta_1x_1v_1 - (\mu_1+\eta_1)l_1)\\ &+ \frac{\mu_1+\eta_1}{\eta_1}\left(1-\frac{\bar{y}_1}{y_1}\right)(\eta_1l_1 - a_1y_1) + \beta_2x_1v_2 - (\mu_2+\eta_2)l_2 + \frac{\mu_2+\eta_2}{\eta_2}(\eta_2l_2 - a_2y_2)\\ &+ \frac{k_3\eta_3(\mu_1+\eta_1)}{k_1\eta_1(\mu_3+\eta_3)}\left(1-\frac{\bar{x}_2}{x_2}\right)(\lambda_2 - d_2x_2 - (1-p)\beta_3x_2v_1)\\ &+ \frac{k_3\eta_3(\mu_1+\eta_1)}{k_1\eta_1(\mu_3+\eta_3)}\left(1-\frac{\bar{l}_3}{l_3}\right)((1-p)\beta_3x_2v_1 - (\mu_3+\eta_3)l_3)\\ &+ \frac{k_3(\mu_1+\eta_1)}{k_1\eta_1}\left(1-\frac{\bar{y}_3}{y_3}\right)(\eta_3l_3 - a_3y_3) + \frac{(\mu_1+\eta_1)}{k_1\eta_1}\left(1-\frac{\bar{v}_1}{v_1}\right)(k_1a_1y_1 + k_3a_3y_3 - c_1v_1)\\ &+ \frac{(\mu_2+\eta_2)}{k_2\eta_2}(k_2a_2y_2 - c_2v_2).\end{aligned}$$

By rearranging and combining like terms, we obtain

$$\begin{aligned}\frac{d\bar{\mathcal{F}}}{dt} &= \left(1-\frac{\bar{x}_1}{x_1}\right)(\lambda_1 - d_1x_1) + p\beta_1\bar{x}_1v_1 + \beta_2\bar{x}_1v_2 - p\beta_1x_1v_1\frac{\bar{l}_1}{l_1} + (\mu_1+\eta_1)\bar{l}_1 - (\mu_1+\eta_1)l_1\frac{\bar{y}_1}{y_1}\\ &+ \frac{\mu_1+\eta_1}{\eta_1}a_1\bar{y}_1 + \frac{k_3\eta_3(\mu_1+\eta_1)}{k_1\eta_1(\mu_3+\eta_3)}\left(1-\frac{\bar{x}_2}{x_2}\right)(\lambda_2 - d_2x_2) + (1-p)\frac{k_3\eta_3(\mu_1+\eta_1)}{k_1\eta_1(\mu_3+\eta_3)}\beta_3\bar{x}_2v_1\\ &- (1-p)\frac{k_3\eta_3(\mu_1+\eta_1)}{k_1\eta_1(\mu_3+\eta_3)}\beta_3x_2v_1\frac{\bar{l}_3}{l_3} + \frac{k_3\eta_3(\mu_1+\eta_1)}{k_1\eta_1}\bar{l}_3\\ &- \frac{k_3\eta_3(\mu_1+\eta_1)}{k_1\eta_1}l_3\frac{\bar{y}_3}{y_3} + \frac{k_3(\mu_1+\eta_1)}{k_1\eta_1}a_3\bar{y}_3 - \frac{(\mu_1+\eta_1)}{k_1\eta_1}c_1v_1\\ &- \frac{(\mu_1+\eta_1)}{\eta_1}a_1y_1\frac{\bar{v}_1}{v_1} - \frac{k_3(\mu_1+\eta_1)}{k_1\eta_1}a_3y_3\frac{\bar{v}_1}{v_1} + \frac{(\mu_1+\eta_1)}{k_1\eta_1}c_1\bar{v}_1 - \frac{(\mu_2+\eta_2)}{k_2\eta_2}c_2v_2.\end{aligned}$$

Utilizing the equilibrium conditions

$$\lambda_1 = d_1\bar{x}_1 + p\beta_1\bar{x}_1\bar{v}_1,\ \lambda_2 = d_2\bar{x}_2 + (1-p)\beta_3\bar{x}_2\bar{v}_1,\ k_1a_1\bar{y}_1 + k_3a_3\bar{y}_3 = c_1\bar{v}_1,$$
$$p\beta_1\bar{x}_1\bar{v}_1 = (\mu_1+\eta_1)\bar{l}_1, \eta_1\bar{l}_1 = a_1\bar{y}_1,\ (1-p)\beta_3\bar{x}_2\bar{v}_1 = (\mu_3+\eta_3)\bar{l}_3, \eta_3\bar{l}_3 = a_3\bar{y}_3,$$

we get

$$a_1\bar{y}_1 = \eta_1\bar{l}_1 = \frac{\eta_1 p}{(\mu_1+\eta_1)}\beta_1\bar{x}_1\bar{v}_1, a_3\bar{y}_3 = \eta_3\bar{l}_3 = \frac{(1-p)\eta_3}{(\mu_3+\eta_3)}\beta_3\bar{x}_2\bar{v}_1.$$

and

$$
\begin{aligned}
\frac{d\bar{\mathcal{F}}}{dt} &= \left(1-\frac{\bar{x}_1}{x_1}\right)(d_1\bar{x}_1 - d_1x_1) + p\beta_1\bar{x}_1\bar{v}_1\left(1-\frac{\bar{x}_1}{x_1}\right) - p\beta_1x_1v_1\frac{\bar{l}_1}{l_1} + p\beta_1\bar{x}_1\bar{v}_1 - p\beta_1\bar{x}_1\bar{v}_1\frac{\bar{y}_1}{y_1}\frac{l_1}{\bar{l}_1} \\
&\quad + p\beta_1\bar{x}_1\bar{v}_1 + \frac{k_3\eta_3(\mu_1+\eta_1)}{k_1\eta_1(\mu_3+\eta_3)}\left(1-\frac{\bar{x}_2}{x_2}\right)(d_2\bar{x}_2 - d_2x_2) + (1-p)\frac{k_3\eta_3(\mu_1+\eta_1)}{k_1\eta_1(\mu_3+\eta_3)}\beta_3\bar{x}_2\bar{v}_1\left(1-\frac{\bar{x}_2}{x_2}\right) \\
&\quad - (1-p)\frac{k_3\eta_3(\mu_1+\eta_1)}{k_1\eta_1(\mu_3+\eta_3)}\beta_3\bar{x}_2\bar{v}_1\frac{x_2v_1\bar{l}_3}{\bar{x}_2\bar{v}_1l_3} + (1-p)\frac{k_3\eta_3(\mu_1+\eta_1)}{k_1\eta_1(\mu_3+\eta_3)}\beta_3\bar{x}_2\bar{v}_1 \\
&\quad - (1-p)\frac{k_3\eta_3(\mu_1+\eta_1)}{k_1\eta_1(\mu_3+\eta_3)}\frac{\bar{y}_3}{y_3}\frac{l_3}{\bar{l}_3}\beta_3\bar{x}_2\bar{v}_1 + (1-p)\frac{k_3\eta_3(\mu_1+\eta_1)}{k_1\eta_1(\mu_3+\eta_3)}\beta_3\bar{x}_2\bar{v}_1 - p\beta_1\bar{x}_1\bar{v}_1\frac{y_1}{\bar{y}_1}\frac{\bar{v}_1}{v_1} \\
&\quad - (1-p)\frac{k_3\eta_3(\mu_1+\eta_1)}{k_1\eta_1(\mu_3+\eta_3)}\beta_3\bar{x}_2\bar{v}_1\frac{y_3}{\bar{y}_3}\frac{\bar{v}_1}{v_1} + p\beta_1\bar{x}_1\bar{v}_1 + (1-p)\frac{k_3\eta_3(\mu_1+\eta_1)}{k_1\eta_1(\mu_3+\eta_3)}\beta_3\bar{x}_2\bar{v}_1 \\
&\quad + \left(\beta_2\bar{x}_1 - \frac{c_2(\mu_2+\eta_2)}{k_2\eta_2}\right)v_2 \\
&= -d_1\frac{(\bar{x}_1-x_1)^2}{x_1} + p\beta_1\bar{x}_1\bar{v}_1\left(4-\frac{\bar{x}_1}{x_1}-\frac{y_1}{\bar{y}_1}\frac{\bar{v}_1}{v_1}-\frac{\bar{y}_1}{y_1}\frac{l_1}{\bar{l}_1}-\frac{x_1v_1}{\bar{x}_1\bar{v}_1}\frac{\bar{l}_1}{l_1}\right) \\
&\quad - d_2\frac{k_3\eta_3(\mu_1+\eta_1)}{k_1\eta_1(\mu_3+\eta_3)}\frac{(\bar{x}_2-x_2)^2}{x_2} + (1-p)\frac{k_3\eta_3(\mu_1+\eta_1)}{k_1\eta_1(\mu_3+\eta_3)}\beta_3\bar{x}_2\bar{v}_1\left(4-\frac{\bar{x}_2}{x_2}-\frac{y_3}{\bar{y}_3}\frac{\bar{v}_1}{v_1}-\frac{\bar{y}_3}{y_3}\frac{l_3}{\bar{l}_3}-\frac{x_2v_1}{\bar{x}_2\bar{v}_1}\frac{\bar{l}_3}{l_3}\right) \\
&\quad + \left(\beta_2\bar{x}_1 - \frac{c_2(\mu_2+\eta_2)}{k_2\eta_2}\right)v_2.
\end{aligned}
$$

Finally we get

$$
\begin{aligned}
\frac{d\bar{\mathcal{F}}}{dt} &= -d_1\frac{(\bar{x}_1-x_1)^2}{x_1} + p\beta_1\bar{x}_1\bar{v}_1\left(4-\frac{\bar{x}_1}{x_1}-\frac{y_1}{\bar{y}_1}\frac{\bar{v}_1}{v_1}-\frac{\bar{y}_1}{y_1}\frac{l_1}{\bar{l}_1}-\frac{x_1v_1}{\bar{x}_1\bar{v}_1}\frac{\bar{l}_1}{l_1}\right) \\
&\quad - d_2\frac{k_3\eta_3(\mu_1+\eta_1)}{k_1\eta_1(\mu_3+\eta_3)}\frac{(\bar{x}_2-x_2)^2}{x_2} + (1-p)\frac{k_3\eta_3(\mu_1+\eta_1)}{k_1\eta_1(\mu_3+\eta_3)}\beta_3\bar{x}_2\bar{v}_1\left(4-\frac{\bar{x}_2}{x_2}-\frac{y_3}{\bar{y}_3}\frac{\bar{v}_1}{v_1}-\frac{\bar{y}_3}{y_3}\frac{l_3}{\bar{l}_3}-\frac{x_2v_1}{\bar{x}_2\bar{v}_1}\frac{\bar{l}_3}{l_3}\right) \\
&\quad + \left(\beta_2\bar{x}_1 - \frac{c_2(\mu_2+\eta_2)}{k_2\eta_2}\right)v_2.
\end{aligned}
$$

We have

$$
\begin{aligned}
\beta_2\bar{x}_1 - \frac{c_2(\mu_2+\eta_2)}{k_2\eta_2} &= \frac{\beta_2\lambda_1}{d_1+p\beta_1\bar{v}_1} - \frac{c_2(\mu_2+\eta_2)}{k_2\eta_2} = \frac{k_2\eta_2\beta_2\lambda_1 - c_2(\mu_2+\eta_2)d_1 - c_2(\mu_2+\eta_2)p\beta_1\bar{v}_1}{k_2\eta_2(d_1+p\beta_1\bar{v}_1)} \\
&= \frac{c_2(\mu_2+\eta_2)d_1\left(\dfrac{k_2\eta_2\beta_2\lambda_1}{c_2(\mu_2+\eta_2)d_1}-1\right)}{k_2\eta_2(d_1+p\beta_1\bar{v}_1)} - \frac{c_2(\mu_2+\eta_2)p\beta_1\bar{v}_1}{k_2\eta_2(d_1+p\beta_1\bar{v}_1)} \\
&= \frac{c_2(\mu_2+\eta_2)d_1\left(\mathcal{R}_1-1\right)}{k_2\eta_2(d_1+p\beta_1\bar{v}_1)} - \frac{c_2(\mu_2+\eta_2)p\beta_1\bar{v}_1}{k_2\eta_2(d_1+p\beta_1\bar{v}_1)} \\
&= \frac{c_2(\mu_2+\eta_2)d_1}{k_2\eta_2(d_1+p\beta_1\bar{v}_1)}\left(\mathcal{R}_1-1-\frac{p\beta_1\bar{v}_1}{d_1}\right).
\end{aligned}
$$

Therefore,

$$
\begin{aligned}
\frac{d\bar{\mathcal{F}}}{dt} &= -d_1\frac{(\bar{x}_1-x_1)^2}{x_1} + p\beta_1\bar{x}_1\bar{v}_1\left(4-\frac{\bar{x}_1}{x_1}-\frac{y_1}{\bar{y}_1}\frac{\bar{v}_1}{v_1}-\frac{\bar{y}_1}{y_1}\frac{l_1}{\bar{l}_1}-\frac{x_1v_1}{\bar{x}_1\bar{v}_1}\frac{\bar{l}_1}{l_1}\right) \\
&\quad - d_2\frac{k_3\eta_3(\mu_1+\eta_1)}{k_1\eta_1(\mu_3+\eta_3)}\frac{(\bar{x}_2-x_2)^2}{x_2} + (1-p)\frac{k_3\eta_3(\mu_1+\eta_1)}{k_1\eta_1(\mu_3+\eta_3)}\beta_3\bar{x}_2\bar{v}_1\left(4-\frac{\bar{x}_2}{x_2}-\frac{y_3}{\bar{y}_3}\frac{\bar{v}_1}{v_1}-\frac{\bar{y}_3}{y_3}\frac{l_3}{\bar{l}_3}-\frac{x_2v_1}{\bar{x}_2\bar{v}_1}\frac{\bar{l}_3}{l_3}\right) \\
&\quad + \frac{c_2(\mu_2+\eta_2)d_1}{k_2\eta_2(d_1+p\beta_1\bar{v}_1)}\left(\mathcal{R}_1-1-\frac{p\beta_1\bar{v}_1}{d_1}\right)v_2.
\end{aligned}
$$

Hence utilizing inequality (12) we obtain $\frac{d\bar{\mathcal{F}}}{dt} \leq 0$ when $\mathcal{R}_1 \leq 1 + \frac{p\beta_1\bar{v}_1}{d_1}$. Further, $\frac{d\bar{\mathcal{F}}}{dt} = 0$ if $(x_1, l_1, y_1, x_2, l_3, y_3, v_1) = \left(\bar{x}_1, \bar{l}_1, \bar{y}_1, \bar{x}_2, \bar{l}_3, \bar{y}_3, \bar{v}_1\right)$ and

$$\left(\mathcal{R}_1 - 1 - \frac{p\beta_1\bar{v}_1}{d_1}\right) v_2 = 0.$$

We have two cases:

- $\mathcal{R}_1 < 1 + \frac{p\beta_1\bar{v}_1}{d_1}$. Then $v_2 = 0$, and hence $\dot{v}_2 = 0$ and from Equation (10) we have $0 = \dot{v}_2 = k_2 a_2 y_2 = 0$ and thus $y_2(t) = 0$. From Equation (5) we get $l_2(t) = 0$ for any t. Hence, $\bar{\Omega}' = \left\{\bar{\mathcal{E}}\right\}$.
- $\mathcal{R}_1 = 1 + \frac{p\beta_1\bar{v}_1}{d_1}$. From Equation (1) we have

$$0 = \dot{x}_1 = \lambda_1 - d_1\bar{x}_1 - p\beta_1\bar{x}_1\bar{v}_1 - \beta_2\bar{x}_1 v_2 \Rightarrow v_2(t) = 0.$$

From Equation (10) we get $y_2(t) = 0$ and then $l_2(t) = 0$ for any t. Hence, $\bar{\Omega}' = \left\{\bar{\mathcal{E}}\right\}$.

LIP indicates that $\bar{\mathcal{E}}$ is GAS when $\mathcal{R}_0 > 1$ and $\mathcal{R}_1 \leq 1 + \frac{p\beta_1\bar{v}_1}{d_1}$. □

Proof. Consider a function candidate $\tilde{\mathcal{F}}(x_1, l_1, y_1, l_2, y_2, x_2, l_3, y_3, v_1, v_2)$

$$\begin{aligned}
\tilde{\mathcal{F}} = {} & x_1 - \tilde{x}_1 - \tilde{x}_1 \ln\left(\frac{x_1}{\tilde{x}_1}\right) + l_1 + \frac{\mu_1 + \eta_1}{\eta_1} y_1 + l_2 - \tilde{l}_2 - \tilde{l}_2 \ln\left(\frac{l_2}{\tilde{l}_2}\right) \\
& + \frac{\mu_2 + \eta_2}{\eta_2}\left(y_2 - \tilde{y}_2 - \tilde{y}_2 \ln\left(\frac{y_2}{\tilde{y}_2}\right)\right) + \frac{k_3\eta_3(\mu_1 + \eta_1)}{k_1\eta_1(\mu_3 + \eta_3)}\left(x_2 - \tilde{x}_2 - \tilde{x}_2 \ln\left(\frac{x_2}{\tilde{x}_2}\right)\right) + \frac{k_3\eta_3(\mu_1 + \eta_1)}{k_1\eta_1(\mu_3 + \eta_3)} l_3 \\
& + \frac{k_3(\mu_1 + \eta_1)}{k_1\eta_1} y_3 + \frac{(\mu_1 + \eta_1)}{k_1\eta_1} v_1 + \frac{(\mu_2 + \eta_2)}{k_2\eta_2}\left(v_2 - \tilde{v}_2 - \tilde{v}_2 \ln\left(\frac{v_2}{\tilde{v}_2}\right)\right).
\end{aligned}$$

We calculate $\frac{d\tilde{\mathcal{F}}}{dt}$ as:

$$\begin{aligned}
\frac{d\tilde{\mathcal{F}}}{dt} = {} & \left(1 - \frac{\tilde{x}_1}{x_1}\right)(\lambda_1 - d_1 x_1 - p\beta_1 x_1 v_1 - \beta_2 x_1 v_2) + p\beta_1 x_1 v_1 - (\mu_1 + \eta_1) l_1 + \frac{\mu_1 + \eta_1}{\eta_1}(\eta_1 l_1 - a_1 y_1) \\
& + \left(1 - \frac{\tilde{l}_2}{l_2}\right)(\beta_2 x_1 v_2 - (\mu_2 + \eta_2) l_2) + \frac{\mu_2 + \eta_2}{\eta_2}\left(1 - \frac{\tilde{y}_2}{y_2}\right)(\eta_2 l_2 - a_2 y_2) \\
& + \frac{k_3\eta_3(\mu_1 + \eta_1)}{k_1\eta_1(\mu_3 + \eta_3)}\left(1 - \frac{\tilde{x}_2}{x_2}\right)(\lambda_2 - d_2 x_2 - (1 - p)\beta_3 x_2 v_1) \\
& + \frac{k_3\eta_3(\mu_1 + \eta_1)}{k_1\eta_1(\mu_3 + \eta_3)}((1 - p)\beta_3 x_2 v_1 - (\mu_3 + \eta_3) l_3) + \frac{k_3(\mu_1 + \eta_1)}{k_1\eta_1}(\eta_3 l_3 - a_3 y_3) \\
& + \frac{(\mu_1 + \eta_1)}{k_1\eta_1}(k_1 a_1 y_1 + k_3 a_3 y_3 - c_1 v_1) + \frac{(\mu_2 + \eta_2)}{k_2\eta_2}\left(1 - \frac{\tilde{v}_2}{v_2}\right)(k_2 a_2 y_2 - c_2 v_2).
\end{aligned}$$

By rearranging and combining like terms, we obtain:

$$\begin{aligned}\frac{d\tilde{\mathcal{F}}}{dt} &= \left(1-\frac{\tilde{x}_1}{x_1}\right)(\lambda_1 - d_1 x_1) + p\beta_1\tilde{x}_1 v_1 + \beta_2\tilde{x}_1 v_2 \\ &- \frac{\tilde{l}_2}{l_2}\beta_2 x_1 v_2 + (\mu_2+\eta_2)\tilde{l}_2 - (\mu_2+\eta_2)l_2\frac{\tilde{y}_2}{y_2} + \frac{\mu_2+\eta_2}{\eta_2}a_2\tilde{y}_2 \\ &+ \frac{k_3\eta_3(\mu_1+\eta_1)}{k_1\eta_1(\mu_3+\eta_3)}\left(1-\frac{\tilde{x}_2}{x_2}\right)(\lambda_2 - d_2 x_2) + (1-p)\frac{k_3\eta_3(\mu_1+\eta_1)}{k_1\eta_1(\mu_3+\eta_3)}\beta_3\tilde{x}_2 v_1 \\ &- \frac{(\mu_1+\eta_1)}{k_1\eta_1}c_1 v_1 - \frac{(\mu_2+\eta_2)}{k_2\eta_2}c_2 v_2 - \frac{(\mu_2+\eta_2)}{\eta_2}\frac{\tilde{v}_2}{v_2}a_2 y_2 + \frac{(\mu_2+\eta_2)}{k_2\eta_2}c_2\tilde{v}_2.\end{aligned}$$

By using the conditions of $\tilde{\mathcal{E}}$,

$$\lambda_1 = d_1\tilde{x}_1 + \beta_2\tilde{x}_1\tilde{v}_2,\ \beta_2\tilde{x}_1\tilde{v}_2 = (\mu_2+\eta_2)\tilde{l}_2, \eta_2\tilde{l}_2 = a_2\tilde{y}_2,\ \lambda_2 = d_2\tilde{x}_2,\ k_2 a_2\tilde{y}_2 = c_2\tilde{v}_2,$$

we obtain

$$\begin{aligned}\frac{d\tilde{\mathcal{F}}}{dt} &= -d_1\frac{(\tilde{x}_1 - x_1)^2}{x_1} + \beta_2\tilde{x}_1\tilde{v}_2 - \beta_2\tilde{x}_1\tilde{v}_2\frac{\tilde{x}_1}{x_1} + p\beta_1\tilde{x}_1 v_1 \\ &- \beta_2\tilde{x}_1\tilde{v}_2\frac{x_1 v_2\tilde{l}_2}{\tilde{x}_1\tilde{v}_2 l_2} + \beta_2\tilde{x}_1\tilde{v}_2 - \beta_2\tilde{x}_1\tilde{v}_2\frac{l_2}{\tilde{l}_2}\frac{\tilde{y}_2}{y_2} + \beta_2\tilde{x}_1\tilde{v}_2 \\ &- \frac{k_3\eta_3(\mu_1+\eta_1)}{k_1\eta_1(\mu_3+\eta_3)}d_2\frac{(\tilde{x}_2 - x_2)^2}{x_2} + (1-p)\frac{k_3\eta_3(\mu_1+\eta_1)}{k_1\eta_1(\mu_3+\eta_3)}\beta_3\tilde{x}_2 v_1 \\ &- \frac{(\mu_1+\eta_1)}{k_1\eta_1}c_1 v_1 - \beta_2\tilde{x}_1\tilde{v}_2\frac{\tilde{v}_2}{v_2}\frac{y_2}{\tilde{y}_2} + \beta_2\tilde{x}_1\tilde{v}_2.\end{aligned}$$

Finally we get

$$\begin{aligned}\frac{d\tilde{\mathcal{F}}}{dt} &= -d_1\frac{(\tilde{x}_1 - x_1)^2}{x_1} - \frac{k_3\eta_3(\mu_1+\eta_1)}{k_1\eta_1(\mu_3+\eta_3)}d_2\frac{(\tilde{x}_2 - x_2)^2}{x_2} + \beta_2\tilde{x}_1\tilde{v}_2\left(4 - \frac{\tilde{x}_1}{x_1} - \frac{x_1 v_2}{\tilde{x}_1\tilde{v}_2}\frac{\tilde{l}_2}{l_2} - \frac{l_2}{\tilde{l}_2}\frac{\tilde{y}_2}{y_2} - \frac{y_2}{\tilde{y}_2}\frac{\tilde{v}_2}{v_2}\right) \\ &+ \left(p\beta_1\tilde{x}_1 + (1-p)\frac{k_3\eta_3(\mu_1+\eta_1)}{k_1\eta_1(\mu_3+\eta_3)}\beta_3\tilde{x}_2 - \frac{(\mu_1+\eta_1)}{k_1\eta_1}c_1\right)v_1.\end{aligned}$$

Furthermore, we have

$$p\beta_1\tilde{x}_1 + (1-p)\frac{k_3\eta_3(\mu_1+\eta_1)}{k_1\eta_1(\mu_3+\eta_3)}\beta_3\tilde{x}_2 - \frac{(\mu_1+\eta_1)}{k_1\eta_1}c_1 = \frac{c_1(\mu_1+\eta_1)}{k_1\eta_1}\left(\frac{\mathcal{R}_{01}}{\mathcal{R}_1} + \mathcal{R}_{02} - 1\right).$$

Then we get

$$\begin{aligned}\frac{d\tilde{\mathcal{F}}}{dt} &= -d_1\frac{(\tilde{x}_1 - x_1)^2}{x_1} - \frac{k_3\eta_3(\mu_1+\eta_1)}{k_1\eta_1(\mu_3+\eta_3)}d_2\frac{(\tilde{x}_2 - x_2)^2}{x_2} + \beta_2\tilde{x}_1\tilde{v}_2\left(4 - \frac{\tilde{x}_1}{x_1} - \frac{x_1 v_2}{\tilde{x}_1\tilde{v}_2}\frac{\tilde{l}_2}{l_2} - \frac{l_2}{\tilde{l}_2}\frac{\tilde{y}_2}{y_2} - \frac{y_2}{\tilde{y}_2}\frac{\tilde{v}_2}{v_2}\right) \\ &+ \frac{c_1(\mu_1+\eta_1)}{k_1\eta_1}\left(\frac{\mathcal{R}_{01}}{\mathcal{R}_1} + \mathcal{R}_{02} - 1\right)v_1.\end{aligned}$$

If $\dfrac{\mathcal{R}_{01}}{\mathcal{R}_1} + \mathcal{R}_{02} \le 1$, then using inequality (12) we obtain $\dfrac{d\tilde{\mathcal{F}}}{dt} \le 0$, where $\dfrac{d\tilde{\mathcal{F}}}{dt} = 0$ occurs at $x_1 = \tilde{x}_1$, $x_2 = \tilde{x}_2$, $l_2 = \tilde{l}_2$, $y_2 = \tilde{y}_2$, $v_2 = \tilde{v}_2$, and

$$\left(\frac{\mathcal{R}_{01}}{\mathcal{R}_1} + \mathcal{R}_{02} - 1\right)v_1 = 0. \tag{B8}$$

We have two cases:

- $\frac{\mathcal{R}_{01}}{\mathcal{R}_1} + \mathcal{R}_{02} = 1$, then from Equation (6) we have

$$0 = \dot{x}_2 = \lambda_2 - d_2\tilde{x}_2 - (1-p)\beta_3\tilde{x}_2 v_1 = -(1-p)\beta_3\tilde{x}_2 v_1 \Longrightarrow v_1(t) = 0, \text{ for any } t,$$

and from Equation (9) we have then

$$0 = \dot{v}_1 = k_1 a_1 y_1 + k_3 a_3 y_3 \Longrightarrow y_1(t) = y_3(t) = 0 \text{ for any } t. \tag{B9}$$

From Equations (3) and (8) we get $l_1(t) = l_3(t) = 0$ for any t. Hence, $\tilde{\Omega}' = \left\{\tilde{\mathcal{E}}\right\}$.

- $\frac{\mathcal{R}_{01}}{\mathcal{R}_1} + \mathcal{R}_{02} < 1$, then $v_1(t) = 0$ and from Equation (B9) we get $y_1(t) = y_3(t) = 0$ and consequently, $l_1(t) = l_3(t) = 0$ for any t. Hence, $\tilde{\Omega}' = \left\{\tilde{\mathcal{E}}\right\}$.

LIP reveals that $\tilde{\mathcal{E}}$ is GAS when $\frac{\mathcal{R}_{01}}{\mathcal{R}_1} + \mathcal{R}_{02} \leq 1$ and $\mathcal{R}_1 > 1$. □

Proof. Let a function $\mathcal{F}^*(x_1, l_1, y_1, l_2, y_2, x_2, l_3, y_3, v_1, v_2)$ as

$$\begin{aligned}
\mathcal{F}^* = {} & x_1 - x_1^* - x_1^* \ln\left(\frac{x_1}{x_1^*}\right) + l_1 - l_1^* - l_1^* \ln\left(\frac{l_1}{l_1^*}\right) + \frac{\mu_1+\eta_1}{\eta_1}\left(y_1 - y_1^* - y_1^* \ln\left(\frac{y_1}{y_1^*}\right)\right) \\
& + l_2 - l_2^* - l_2^* \ln\left(\frac{l_2}{l_2^*}\right) + \frac{\mu_2+\eta_2}{\eta_2}\left(y_2 - y_2^* - y_2^* \ln\left(\frac{y_2}{y_2^*}\right)\right) \\
& + \frac{k_3\eta_3(\mu_1+\eta_1)}{k_1\eta_1(\mu_3+\eta_3)}\left(x_2 - x_2^* - x_2^* \ln\left(\frac{x_2}{x_2^*}\right)\right) + \frac{k_3\eta_3(\mu_1+\eta_1)}{k_1\eta_1(\mu_3+\eta_3)}\left(l_3 - l_3^* - l_3^* \ln\left(\frac{l_3}{l_3^*}\right)\right) \\
& + \frac{k_3(\mu_1+\eta_1)}{k_1\eta_1}\left(y_3 - y_3^* - y_3^* \ln\left(\frac{y_3}{y_3^*}\right)\right) + \frac{\mu_1+\eta_1}{k_1\eta_1}\left(v_1 - v_1^* - v_1^* \ln\left(\frac{v_1}{v_1^*}\right)\right) \\
& + \frac{\mu_2+\eta_2}{k_2\eta_2}\left(v_2 - v_2^* - v_2^* \ln\left(\frac{v_2}{v_2^*}\right)\right).
\end{aligned}$$

Calculating $\frac{d\mathcal{F}^*}{dt}$ as:

$$\begin{aligned}
\frac{d\mathcal{F}^*}{dt} = {} & \left(1 - \frac{x_1^*}{x_1}\right)(\lambda_1 - d_1 x_1 - p\beta_1 x_1 v_1 - \beta_2 x_1 v_2) + \left(1 - \frac{l_1^*}{l_1}\right)(p\beta_1 x_1 v_1 - (\mu_1+\eta_1) l_1) \\
& + \frac{\mu_1+\eta_1}{\eta_1}\left(1 - \frac{y_1^*}{y_1}\right)(\eta_1 l_1 - a_1 y_1) + \left(1 - \frac{l_2^*}{l_2}\right)(\beta_2 x_1 v_2 - (\mu_2+\eta_2) l_2) \\
& + \frac{\mu_2+\eta_2}{\eta_2}\left(1 - \frac{y_2^*}{y_2}\right)(\eta_2 l_2 - a_2 y_2) + \frac{k_3\eta_3(\mu_1+\eta_1)}{k_1\eta_1(\mu_3+\eta_3)}\left(1 - \frac{x_2^*}{x_2}\right)(\lambda_2 - d_2 x_2 - (1-p)\beta_3 x_2 v_1) \\
& + \frac{k_3\eta_3(\mu_1+\eta_1)}{k_1\eta_1(\mu_3+\eta_3)}\left(1 - \frac{l_3^*}{l_3}\right)((1-p)\beta_3 x_2 v_1 - (\mu_3+\eta_3) l_3) \\
& + \frac{k_3(\mu_1+\eta_1)}{k_1\eta_1}\left(1 - \frac{y_3^*}{y_3}\right)(\eta_3 l_3 - a_3 y_3) + \frac{\mu_1+\eta_1}{k_1\eta_1}\left(1 - \frac{v_1^*}{v_1}\right)(k_1 a_1 y_1 + k_3 a_3 y_3 - c_1 v_1) \\
& + \frac{\mu_2+\eta_2}{k_2\eta_2}\left(1 - \frac{v_2^*}{v_2}\right)(k_2 a_2 y_2 - c_2 v_2).
\end{aligned}$$

By rearranging and combining like terms, we obtain

$$\begin{aligned}\frac{d\mathcal{F}^*}{dt} &= \left(1-\frac{x_1^*}{x_1}\right)(\lambda_1 - d_1x_1) + p\beta_1x_1^*v_1 + \beta_2x_1^*v_2 - p\beta_1x_1v_1\frac{l_1^*}{l_1} + (\mu_1+\eta_1)l_1^* \\ &- (\mu_1+\eta_1)l_1\frac{y_1^*}{y_1} + \frac{\mu_1+\eta_1}{\eta_1}a_1y_1^* - \beta_2x_1v_2\frac{l_2^*}{l_2} + (\mu_2+\eta_2)l_2^* - (\mu_2+\eta_2)l_2\frac{y_2^*}{y_2} + \frac{\mu_2+\eta_2}{\eta_2}a_2y_2^* \\ &+ \frac{k_3\eta_3(\mu_1+\eta_1)}{k_1\eta_1(\mu_3+\eta_3)}\left(1-\frac{x_2^*}{x_2}\right)(\lambda_2 - d_2x_2) + (1-p)\frac{k_3\eta_3(\mu_1+\eta_1)}{k_1\eta_1(\mu_3+\eta_3)}\beta_3x_2^*v_1 \\ &- (1-p)\frac{k_3\eta_3(\mu_1+\eta_1)}{k_1\eta_1(\mu_3+\eta_3)}\beta_3x_2v_1\frac{l_3^*}{l_3} + \frac{k_3\eta_3(\mu_1+\eta_1)}{k_1\eta_1}l_3^* \\ &- \frac{k_3\eta_3(\mu_1+\eta_1)}{k_1\eta_1}l_3\frac{y_3^*}{y_3} + \frac{k_3(\mu_1+\eta_1)}{k_1\eta_1}a_3y_3^* \\ &- \frac{(\mu_1+\eta_1)}{k_1\eta_1}c_1v_1 - \frac{(\mu_1+\eta_1)}{\eta_1}a_1y_1\frac{v_1^*}{v_1} - \frac{k_3(\mu_1+\eta_1)}{k_1\eta_1}a_3y_3\frac{v_1^*}{v_1} + \frac{(\mu_1+\eta_1)}{k_1\eta_1}c_1v_1^* \\ &- \frac{(\mu_2+\eta_2)}{k_2\eta_2}c_2v_2 - \frac{(\mu_2+\eta_2)}{\eta_2}a_2y_2\frac{v_2^*}{v_2} + \frac{(\mu_2+\eta_2)}{k_2\eta_2}c_2v_2^*.\end{aligned}$$

Utilizing the equilibrium conditions

$$\begin{aligned}&\lambda_1 = d_1x_1^* + p\beta_1x_1^*v_1^* + \beta_2x_1^*v_2^*,\ p\beta_1x_1^*v_1^* = (\mu_1+\eta_1)l_1^*,\ \eta_1l_1^* = a_1y_1^*,\ \beta_2x_1^*v_2^* = (\mu_2+\eta_2)l_2^*, \\ &\eta_2l_2^* = a_2y_2^*,\ \lambda_2 = d_2x_2^* + (1-p)\beta_3x_2^*v_1^*,\ (1-p)\beta_3x_2^*v_1^* = (\mu_3+\eta_3)l_3^*,\ \eta_3l_3^* = a_3y_3^*, \\ &c_1v_1^* = k_1a_1y_1^* + k_3a_3y_3^*,\ c_2v_2^* = k_2a_2y_2^*,\end{aligned}$$

we get

$$\begin{aligned}a_1y_1^* &= \frac{p\eta_1}{(\mu_1+\eta_1)}\beta_1x_1^*v_1^*,\ a_2y_2^* = \frac{\eta_2}{(\mu_2+\eta_2)}\beta_2x_1^*v_2^*, \\ a_3y_3^* &= \frac{(1-p)\eta_3}{(\mu_3+\eta_3)}\beta_3x_2^*v_1^*,\ l_1^* = \frac{p}{(\mu_1+\eta_1)}\beta_1x_1^*v_1^*, \\ l_2^* &= \frac{1}{(\mu_2+\eta_2)}\beta_2x_1^*v_2^*,\ l_3^* = \frac{1-p}{(\mu_3+\eta_3)}\beta_3x_2^*v_1^*, \\ c_1v_1^* &= \frac{pk_1\eta_1}{(\mu_1+\eta_1)}\beta_1x_1^*v_1^* + \frac{(1-p)k_3\eta_3}{(\mu_3+\eta_3)}\beta_3x_2^*v_1^*, \\ c_2v_2^* &= \frac{k_2\eta_2}{(\mu_2+\eta_2)}\beta_2x_1^*v_2^*.\end{aligned}$$

Therefore,

$$\begin{aligned}\frac{d\mathcal{F}^*}{dt} &= \left(1-\frac{x_1^*}{x_1}\right)(d_1x_1^*-d_1x_1)+p\beta_1x_1^*v_1^*+\beta_2x_1^*v_2^*-p\beta_1x_1^*v_1^*\frac{x_1^*}{x_1}-\beta_2x_1^*v_2^*\frac{x_1^*}{x_1}\\ &-p\beta_1x_1^*v_1^*\frac{x_1v_1l_1^*}{x_1^*v_1^*l_1}+p\beta_1x_1^*v_1^*-p\beta_1x_1^*v_1^*\frac{l_1}{l_1^*}\frac{y_1^*}{y_1}+p\beta_1x_1^*v_1^*-\beta_2x_1^*v_2^*\frac{x_1v_2l_2^*}{x_1^*v_2^*l_2}\\ &+\beta_2x_1^*v_2^*-\beta_2x_1^*v_2^*\frac{l_2}{l_2^*}\frac{y_2^*}{y_2}+\beta_2x_1^*v_2^*+\frac{k_3\eta_3(\mu_1+\eta_1)}{k_1\eta_1(\mu_3+\eta_3)}\left(1-\frac{x_2^*}{x_2}\right)(d_2x_2^*-d_2x_2)\\ &+(1-p)\frac{k_3\eta_3(\mu_1+\eta_1)}{k_1\eta_1(\mu_3+\eta_3)}\beta_3x_2^*v_1^*-(1-p)\frac{k_3\eta_3(\mu_1+\eta_1)}{k_1\eta_1(\mu_3+\eta_3)}\beta_3x_2^*v_1^*\frac{x_2^*}{x_2}\\ &-(1-p)\frac{k_3\eta_3(\mu_1+\eta_1)}{k_1\eta_1(\mu_3+\eta_3)}\beta_3x_2^*v_1^*\frac{x_2v_1l_3^*}{x_2^*v_1^*l_3}+(1-p)\frac{k_3\eta_3(\mu_1+\eta_1)}{k_1\eta_1(\mu_3+\eta_3)}\beta_3x_2^*v_1^*\\ &-(1-p)\frac{k_3\eta_3(\mu_1+\eta_1)}{k_1\eta_1(\mu_3+\eta_3)}\beta_3x_2^*v_1^*\frac{l_3}{l_3^*}\frac{y_3^*}{y_3}+(1-p)\frac{k_3\eta_3(\mu_1+\eta_1)}{k_1\eta_1(\mu_3+\eta_3)}\beta_3x_2^*v_1^*\\ &-p\beta_1x_1^*v_1^*\frac{y_1}{y_1^*}\frac{v_1^*}{v_1}-(1-p)\frac{k_3\eta_3(\mu_1+\eta_1)}{k_1\eta_1(\mu_3+\eta_3)}\beta_3x_2^*v_1^*\frac{y_3}{y_3^*}\frac{v_1^*}{v_1}+p\beta_1x_1^*v_1^*\\ &+(1-p)\frac{k_3\eta_3(\mu_1+\eta_1)}{k_1\eta_1(\mu_3+\eta_3)}\beta_3x_2^*v_1^*-\beta_2x_1^*v_2^*\frac{y_2}{y_2^*}\frac{v_2^*}{v_2}+\beta_2x_1^*v_2^*.\end{aligned}$$

Finally we get

$$\begin{aligned}\frac{d\mathcal{F}^*}{dt} &= -d_1\frac{(x_1-x_1^*)^2}{x_1}-\frac{k_3\eta_3(\mu_1+\eta_1)}{k_1\eta_1(\mu_3+\eta_3)}d_2\frac{(x_2-x_2^*)^2}{x_2}\\ &+p\beta_1x_1^*v_1^*\left(4-\frac{x_1^*}{x_1}-\frac{y_1}{y_1^*}\frac{v_1^*}{v_1}-\frac{l_1}{l_1^*}\frac{y_1^*}{y_1}-\frac{x_1v_1}{x_1^*v_1^*}\frac{l_1^*}{l_1}\right)\\ &+\beta_2x_1^*v_2^*\left(4-\frac{x_1^*}{x_1}-\frac{y_2}{y_2^*}\frac{v_2^*}{v_2}-\frac{l_2}{l_2^*}\frac{y_2^*}{y_2}-\frac{x_1v_2}{x_1^*v_2^*}\frac{l_2^*}{l_2}\right)\\ &+(1-p)\frac{k_3\eta_3(\mu_1+\eta_1)}{k_1\eta_1(\mu_3+\eta_3)}\beta_3x_2^*v_1^*\left(4-\frac{x_2^*}{x_2}-\frac{y_3}{y_3^*}\frac{v_1^*}{v_1}-\frac{l_3}{l_{3*}}\frac{y_3^*}{y_3}-\frac{x_2v_1}{x_2^*v_1^*}\frac{l_3^*}{l_3}\right).\end{aligned}$$

Therefore, using inequality (12) we get $\frac{d\mathcal{F}^*}{dt}\leq 0$ for all $x_1,l_1,y_1,l_2,y_2,x_2,l_3,y_3,v_1,v_2>0$. Moreover, $\frac{d\mathcal{F}^*}{dt}=0$ when $(x_1,l_1,y_1,l_2,y_2,x_2,l_3,y_3,v_1,v_2)=(x_1^*,l_1^*,y_1^*,l_2^*,y_2^*,x_2^*,l_3^*,y_3^*,v_1^*,v_2^*)$. Therefore, $\Omega^{*\prime}=\{\mathcal{E}^*\}$. Applying LIP we get that $\mathcal{E}^*$ is GAS. □